SUPPORTING INFORMATION FOR:

Sierra-Montoya, M., Muñoz-Liesa, J., Pérez-Sánchez, L.À., de Tomás-Pascual, A. & Madrid-López, C. WindTrace: Testing the environmental impacts of wind energy designs with a parametric life cycle inventory model. Journal of Industrial Ecology.

Summary

This supporting information provides additional details on the methods to develop and validate WindTrace, as well as analysis that complement the results in the main text.

1. WindTrace development

WindTrace is an open-source parametrized life-cycle inventory model for wind turbines. The code and simple examples of use can be consulted in GithHub: https://github.com/LIVENlab/WindTrace_public. Table S1 summarises the input data required by the model to run.

1.1. Modelling the material phase

1.1.1. Modelling the foreground

The general approach to model the materials from the turbine and foundations was to adjust first order fitting curves to each material mass versus the power of the turbine. Mass of steel was modelled as a function of the hub height instead of the power capacity, as most of the steel in a wind turbine is contained in the tower. The data was collected from Vestas LCA reports from the period 2011-2023. The reports include the following models:

- 2 MW: V90-2.0 [1], V100-2.0 [2], V110-2.0 [3], V116-2.0 [4], V120-2.0 [5].
- 2.6 MW: V100-2.6 [6].
- 3.0 MW: V90-3.0 [7].
- 3.3 MW: V105-3.3 [8], V112-3.3 [9], V117-3.3 [10], V126-3.3 [11].
- 3.45 MW: V105-3.45 [12], V112-3.45 [13], V117-3.45 [14], V126-3.45 [15], V136-3.45 [16].
- 4.2 MW: V117-4.2 [17], V136-4.2 [18], V150-4.2 [19].
- ≥6.0 MW: V150-6.0 [20], V162-6.2 [21].

Table S1. WindTrace input data.

Parameter	Description	Default value	Overview of its function in WindTrace
Park name	Name of the wind park	No	To name the wind park and wind turbine Brightway2.5 activities
Park power	Total power of the wind park	No	To scale the dimensions of the transformer
Number of turbines	Number of turbines in the wind park	No	To create wind park inventory
Park location	Abbreviation of the country where the turbine is located (ISO 3166-1 alpha-2 codes)	No	To give a location to wind turbine activities in Brightway
Park coordinates	WGS84 coordinates of the wind park (latitude, longitude)	No	To calculate transport distance from manufacturing site
Manufacturer	Name of the manufacturer of the turbines from the following (Vestas, Siemens Gamesa, Enercon, Nordex)	LM Wind	To find the closest manufacturing site of the manufacturer to the wind park
Rotor diameter	Diameter of the rotor (in meters)	No	To calculate distance between turbines needed to model cable length
Turbine rated power	Nominal power of the individual turbines	No	To scale the materials' amounts except for steel
Hub height	Height of the turbine	No	To scale steel mass
Regression adjustment	Steel mass as function of D^2h or Hub height	D^2h	To scale steel mass
Commissioning year	Year when the turbine started the operation	No	To define the turbine manufacturing year and the corresponding recycling share of steel for that year
Recycled steel share	Share of recycled steel in the turbine	Data from Eurofer (2012 – 2021)	Direct input
Electricity mix steel	Electricity mix used to produce steel and chromium steel	Mix according to Eurofer's production data per country	Direct input
Generator type	Use of gearbox and type of generator	Doubly fed induction generator (gearbox)	To scale the amount of rare earth metals in the turbine
Land use permanent intensity	Permanent direct land transformation per MW	3000 m^2/MW	Direct input
Land cover type	Land cover type prior to the turbines' installation	No	Direct input
End-of-life scenario	Selection of end-of-life scenario based on different materials recycling rates	Baseline	Direct input
Lifetime	Lifetime of the turbine (expected, if it has not yet been decommissioned)	20 years	To calculate land occupation, and the electricity production throughout the operation lifetime
Capacity factor	Ratio of average delivered electricity to theoretical maximum electricity production	0.24	To calculate the electricity production throughout the operation lifetime
Attrition rate	Annual rate of efficiency reduction of the turbine due to attrition	0.009	To adjust the annual capacity factor

The materials, their names in Vestas' report, part of the turbine where the material is located and associated background Ecoinvent activities are described in Table S2.

Table S2. Summary of the materials in the LCI of wind turbine, their inclusion in the different parts (turbine or foundations) and the chosen Ecoinvent activity.

Material's name in Vestas reports	Material in WindTrace	Part (Turbine or Foundation)	Ecoinvent v3.9.1 activity
Steel unalloyed, low alloyed	Low alloyed steel	Turbine and foundations	market for steel, low-alloyed*** / market for reinforcing steel
Steel, highly alloyed	Chromium steel	Turbine and foundations	market for steel, chromium steel 18/8
Cast iron	Cast iron	Turbine	market for cast iron
Aluminium and aluminium alloys	Aluminium	Turbine	market for aluminium, wrought alloy
Copper and copper alloys	Copper	Turbine	market for copper, cathode
*Polymer materials**	*Polymer materials**	*Turbine***	-
Thermoplastics	Polyvinyl chloride (PVC)	Turbine	market for polyvinylchloride, bulk polymerised
Elastomers	Rubber	Turbine	market for synthetic rubber
Thermoplastic elastomers	Epoxy resin	Turbine	market for epoxy resin, liquid
Duromers			
Polymeric compounds			
Lacquers and adhesives	Polyurethane (PUR)	Turbine	market for polyurethane, rigid foam
Modified organic materials	Not included	Not included	Not included
Ceramic / glass	Fibreglass****	Turbine	market for glass fibre reinforced plastic, polyamide, injection moulded
Other materials and compounds	Not included	Not included	Not included
Concrete	Concrete	Foundations	market group for concrete, normal
Electrics	Electrics	Turbine	cable production, unspecified
Electronics	Electronics	Turbine	market for electronics, for control units
Magnets			
Lubricants	Lubricating oil	Turbine	market for lubricating oil
Not included	Praseodymium	Turbine	market for praseodymium oxide
Not included	Neodymium	Turbine	market for neodymium oxide
Not included	Dysprosium	Turbine	market for dysprosium oxide
Not included	Terbium	Turbine	market for terbium oxide
Not included	Boron	Turbine	market for boron carbide

*Polymer materials appeared as disaggregated categories in Vestas' reports until 2014. To disaggregate the polymer materials category of the post-2014 reports, we calculated the mean values for each polymer material with data from reports until 2014. Then, we extrapolated the missing data for post-2014 reports. The equivalence between the polymeric categories in Vestas' reports (column: Material's name in Vestas reports) and how they were categorized in WindTrace (column: Material in WindTrace) was done considering the chemical and mechanical properties of the materials.

**Although plastic materials were also described in the foundations of several Vestas' reports, it was not included due to negligible values. Site-cable materials from Vestas' reports were not considered because the inventories refer to a specific wind park design in a particular location in Germany and therefore cannot be extrapolated to other designs and settings.

***Background adjustments were made to the Ecoinvent activity, and instead, tailor-made markets for steel activities were created and used. The background adjustments methods are explained in section 1.1.2.

****Fibreglass is the only material for which manufacturing wastes are included as input materials. The reason is that these wastes add up to 10% of the total fibreglass contained in the blades [22].

Figure S1 shows the fitting curves for the mass of all materials in the wind turbine and the foundations as a function of power. In the case of steel, mass is correlated with hub height. The shaded area corresponds to the mean standard deviation of the residuals.

For those materials where the fitting curve has a high deviation from the origin of coordinates, another fitting curve was built between 0 and 0.8 MW. In those cases, the intersection point between the curves is highlighted with a red dot. Also, the R^2 for those materials with intersection points corresponds to the fitting curve for values >0.8 MW. For all materials, R^2 is above 0.8 except for electronics, fibreglass and lubrication oil, due to outliers, and chromium steel in the foundations due to variability in the input data.

Finally, WindTrace includes material intensities for praseodymium, neodymium, dysprosium, terbium, and boron from Carrara et al. [23]. These intensities, presented in

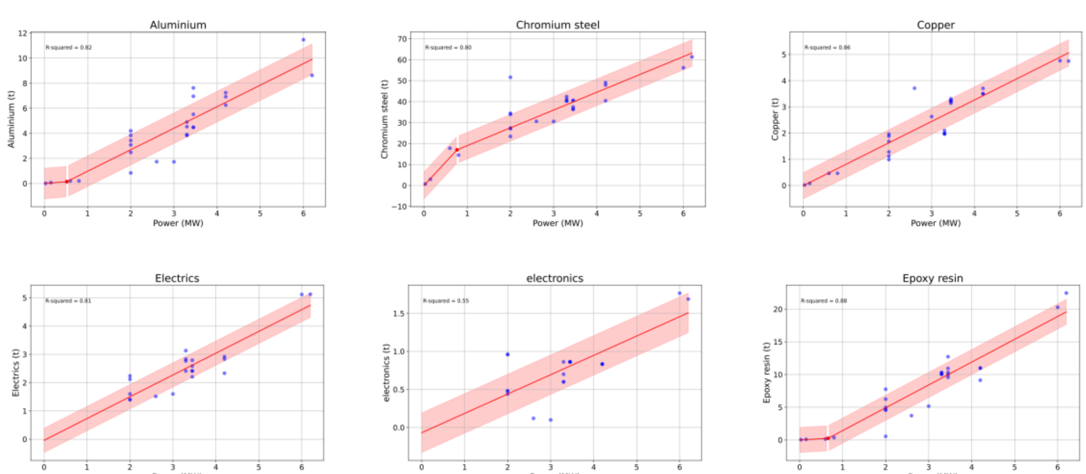

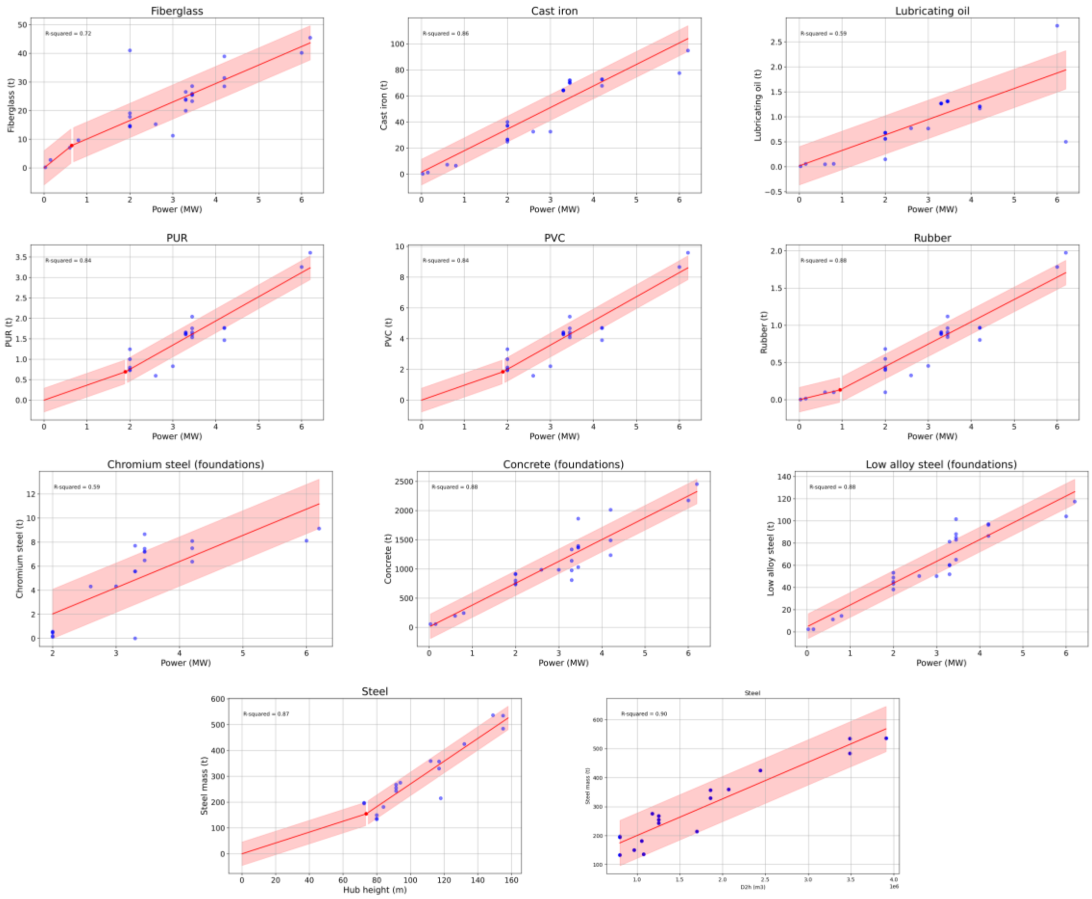

Figure S1. Materials in the turbine and foundations. Steel (turbine) represented as a function of hub height and as a function of D^2h.

Table S3 are assigned according to different combinations of drivetrain (direct drive or gearbox, plus type of generator): Double-Fed Induction Generator (DFIG), Permanent Magnet Synchronous Generator (PMSG) and Electrically Excited Synchronous Generator (EESG). These include:

1) Direct-driven Permanent Magnet Synchronous Generator (dd-pmsg)
2) Gear-boxed Permanent Magnet Synchronous Generator (gb-pmsg)
3) Direct-driven Electrically Excited Synchronous Generator (dd-eesg)
4) Gear-boxed Double-Fed Induction Generator (gb-dfig)

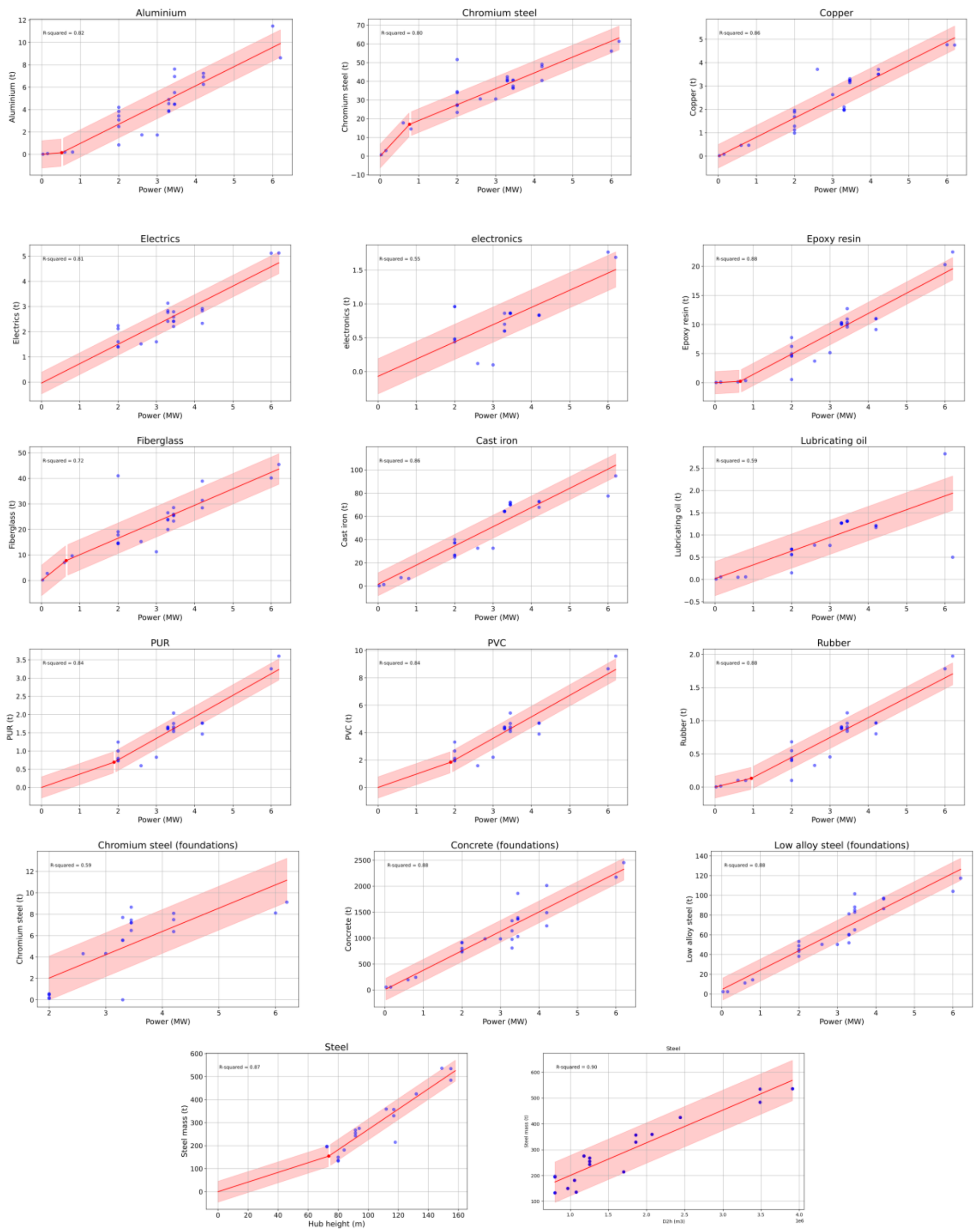

Figure S1. Materials in the turbine and foundations. Steel (turbine) represented as a function of hub height and as a function of D^2h.

Table S3. Rare earth metal material intensities (t/GW) used by WindTrace.

Material	dd-eesg	dd-pmsg	gb-pmsg	gb-dfig
Dysprosium	6	17	6	2
Neodymium	28	180	51	12
Praseodymium	9	35	4	0
Boron	0	6	1	0
Total	**45**	**238**	**61**	**14**

All materials in this section are included as inputs in the inventory using Brightway2.5 [24]. They include a Normal Distribution uncertainty with the interpolation of the fitting curve stored as the 'loc' parameter in the Brightway2.5 inventory and the standard deviation of the residuals stored as the 'scale' values. Rare earth material inputs were not assigned uncertainty due to a lack of data.

1.1.1.1. Alternative approaches

Although materials masses were calculated as a function of power (or hub height in the case of steel) as explained above, other approaches could have been used. Here, we summarize the range of alternatives that were considered and why they were discarded.

- Fibreglass and epoxy as a function of the rotor diameter

Fibreglass and epoxy resin represent a proportion of 58-61% and 21-28% of the total mass of a wind turbine blade, respectively, according to material passports made publicly available by LM Wind Power and Vestas [25,26]. Thus, calculation of their masses as a function of the rotor diameter was tried. However, as shown in Figure S2, the R^2 were 66% and 62%, respectively, less than the 72% and 88% obtained when power was the independent variable.

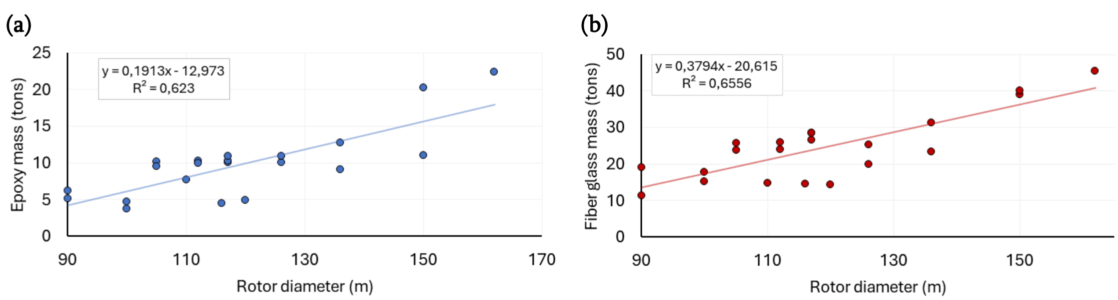

Figure S2. Mass of materials as a function of the rotor diameter for (a) Epoxy resin, and (b) Fibreglass.

- Foundations materials as a function of steel

An alternative approach to calculate the amount of foundation materials was to assess their masses as a function of the steel mass. The idea comes from the fact that the size of the foundations depends partially on the mass it needs to support, which is mostly the mass of the steel tower. The results are shown in Figure S3, where there is a tiny improvement in the R^2 shown for all the materials. This is 0.61 instead of 0.59 for chromium steel, 0.96 instead of 0.88 for concrete and 0.90 instead of 0.88 in the case of steel.

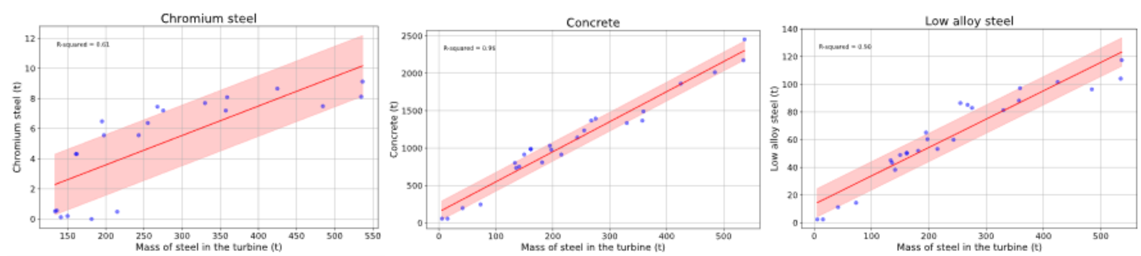

Figure S3. Mass of the materials in the foundations (chromium steel, concrete and low alloy steel) as a function of the mass of steel in the turbine.

The R^2 differences between modelling the foundations as a function of the power as we finally did in the main text and this approach are small. Thus, to further test the accuracy of this alternative approach, we performed a validation of both modelling approaches. We took 18 Vestas turbines as blind samples (a set of datasets employed to model the materials in WindTrace) and modelled the entire turbine with WindTrace using both approaches for the foundations. We then calculated LCIA results for both inventories using ReCiPe 2016 v1.1 midpoint (H) [27]. We also took the original material masses from these 18 Vestas turbines from the official reports and performed LCIAs to them. Finally, we compared the LCIA results from each approach to the LCIA results of original masses to check how much each modelling approach deviates from the original LCIA results. We applied Mean Squared Error (RMSE), Mean Percentage Error (MPE), and R^2 for the comparison. The results of these comparisons are plotted in Figure S4 and Figure S5.

Table S4 shows that when modelling the foundations as a function of the mass of steel, the R^2, RMSE and MPE improves only for 5, 3 and 6 categories, respectively, of a total of 18 categories. There is also a general drop in the MPE, there being 12 negative results with the steel mass approach while in the power approach it is only one. This means that WindTrace is slightly underestimating the impacts with the power approach. Therefore, for most impact categories the validation shows better statistical results using the power approach, and we stick to it to calculate the foundation material masses in WindTrace.

Table S4. LCIA results comparison of two foundations modelling approaches and the LCIA results from the original masses reported by Vestas. The foundation modelling approaches are: (1) as a function of power, and (2) as a function of the mass of steel.

	Foundations as a function of power			Foundations as a function of the mass of steel		
Impact category	R^2	RMSE (%)	MPE (%)	R^2	RMSE (%)	MPE (%)
Climate Change	0.96	6	1.55	0.93	8	-0.82
Ozone Depletion	0.95	6	4.73	0.96	6	3.86
Ionising Radiation	0.96	6	0.84	0.93	9	-1.15
Fine Particulate Matter Formation	0.97	5	0.35	0.96	6	-0.89
Photochemical Oxidant Formation: Ecosystem Quality	0.96	6	0.89	0.94	8	-1.56
Photochemical Oxidant Formation: Human Health	0.96	6	0.89	0.94	8	-1.56
Terrestrial Acidification	0.97	5	0.92	0.97	5	-0.38
Freshwater Eutrophication	0.97	6	0.17	0.96	7	-1.47
Marine Eutrophication	0.93	8	6.31	0.94	7	5.56
Human Toxicity: Cancer	0.92	9	0.68	0.87	13	-1.92
Human Toxicity: Non-cancer	0.95	7	0.25	0.96	7	-0.49
Terrestrial Ecotoxicity	0.96	6	-0.05	0.97	5	-0.36
Freshwater Ecotoxicity	0.95	7	0.39	0.96	7	-0.47
Marine Ecotoxicity	0.96	7	0.36	0.96	6	-0.55
Land Use	0.96	6	0.28	0.94	8	-2.11
Water Use	0.96	6	4.55	0.96	6	3.39
Mineral Resource Scarcity	0.92	10	0.72	0.87	13	-2.11
Fossil Resource Scarcity	0.97	6	1.80	0.95	7	0.02

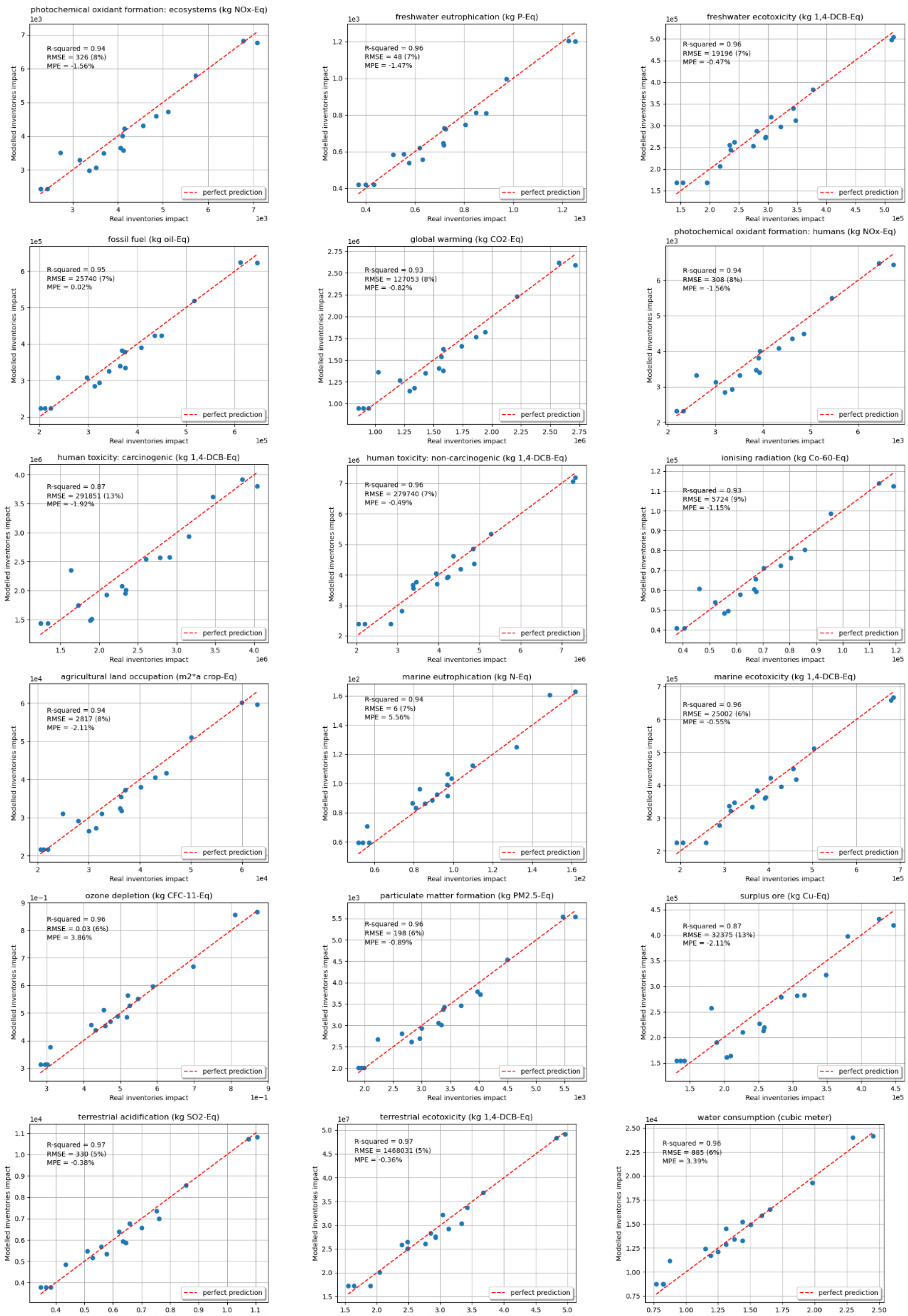

Figure S4. LCIA results comparison between the inventories modelled with WindTrace using the 'mass of steel' approach for the foundations and the inventories using original data from Vestas reports.

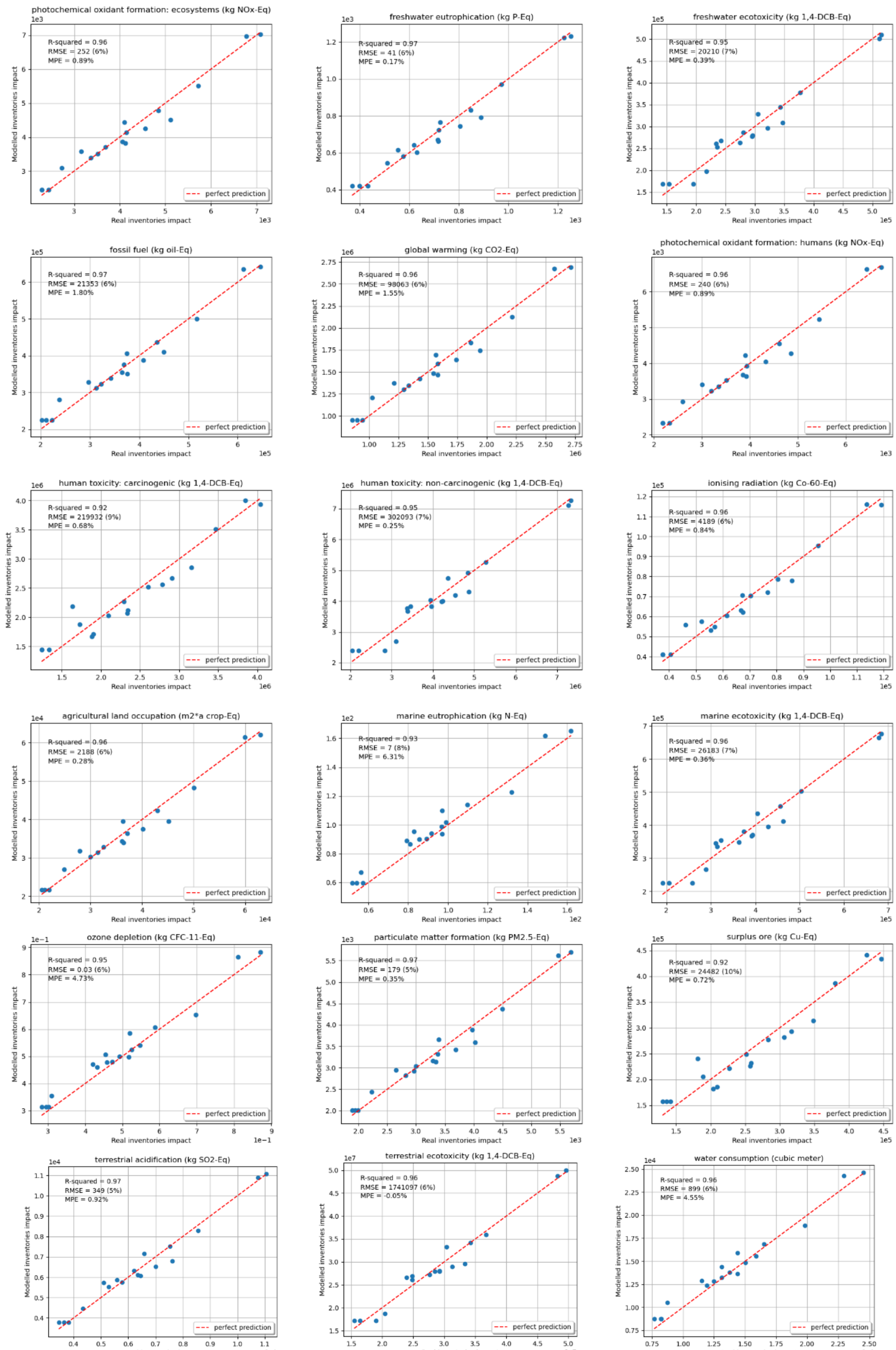
photochemical oxidant formation: ecosystems (kg NOx-Eq)
R-squared = 0.96
RMSE = 252 (6%)
MPE = 0.89%
freshwater eutrophication (kg P-Eq)
R-squared = 0.97
RMSE = 41 (6%)
MPE = 0.17%
freshwater ecotoxicity (kg 1,4-DCB-Eq)
R-squared = 0.95
RMSE = 20210 (7%)
MPE = 0.39%
fossil fuel (kg oil-Eq)
R-squared = 0.97
RMSE = 21353 (6%)
MPE = 1.80%
global warming (kg CO2-Eq)
R-squared = 0.96
RMSE = 98063 (6%)
MPE = 1.55%
photochemical oxidant formation: humans (kg NOx-Eq)
R-squared = 0.96
RMSE = 240 (6%)
MPE = 0.89%
human toxicity: carcinogenic (kg 1,4-DCB-Eq)
R-squared = 0.92
RMSE = 219932 (9%)
MPE = 0.68%
human toxicity: non-carcinogenic (kg 1,4-DCB-Eq)
R-squared = 0.95
RMSE = 302093 (7%)
MPE = 0.25%
ionising radiation (kg Co-60-Eq)
R-squared = 0.96
RMSE = 4189 (6%)
MPE = 0.84%
agricultural land occupation (m2*a crop-Eq)
R-squared = 0.96
RMSE = 2188 (6%)
MPE = 0.28%
marine eutrophication (kg N-Eq)
R-squared = 0.93
RMSE = 7 (8%)
MPE = 6.31%
marine ecotoxicity (kg 1,4-DCB-Eq)
R-squared = 0.96
RMSE = 26183 (7%)
MPE = 0.36%
ozone depletion (kg CFC-11-Eq)
R-squared = 0.95
RMSE = 0.03 (6%)
MPE = 4.73%
particulate matter formation (kg PM2.5-Eq)
R-squared = 0.97
RMSE = 179 (5%)
MPE = 0.35%
surplus ore (kg Cu-Eq)
R-squared = 0.92
RMSE = 24482 (10%)
MPE = 0.72%
terrestrial acidification (kg SO2-Eq)
R-squared = 0.97
RMSE = 349 (5%)
MPE = 0.92%
terrestrial ecotoxicity (kg 1,4-DCB-Eq)
R-squared = 0.96
RMSE = 1741097 (6%)
MPE = -0.05%
water consumption (cubic meter)
R-squared = 0.96
RMSE = 899 (6%)
MPE = 4.55%

Figure S5. LCIA results comparison between the inventories modelled with WindTrace using the 'power' approach for the foundations and the inventories using original data from Vestas reports.

1.1.1.2. Statistical analysis of regression models for materials

This section details the statistical assessment of the linear regression models developed for the wind turbine and foundation materials. This analysis was undertaken to thoroughly understand the inherent uncertainty and appropriateness of the derived fits, which are foundational for subsequent life cycle impact assessments.

For each material, the residuals from the initial linear regression models (material mass vs D^2h for low alloy steel, and vs power for all other materials) were first subjected to a Normality test using the Shapiro-Wilk method. This test is particularly well-suited for evaluating normality with relatively small sample sizes (N), as it has demonstrated high power for this purpose [70]. Table S5 presents the outcomes of these normality tests; a p-value exceeding 0.05 was considered indicative of residual normality. As observed, the normality assumption was declined for the residuals of Low Alloy steel, Fiberglass, Copper, and Lubricating oil. The Q-Q plots for all materials are presented in Figure S6.

Table S5. Normality test results for material regression residuals

Material	Aluminium	Cast iron	Chromium steel (Foundations)	Chromium steel	Concrete (Foundations)	Copper	Electrics	Epoxy resin
Normality Test Result	Accepted (p=0.996)	Accepted (p=0.112)	Accepted (p=0.563)	Accepted (p=0.941)	Accepted (p=0.224)	Declined (p=0.043)	Accepted (p=0.843)	Accepted (p=0.109)
Material	**Low alloy steel (Foundations)**	**Low alloy steel**	**Lubricating oil**	**PUR**	**PVC**	**Rubber**	**electronics**	**Fiberglass**
Normality Test Result	Accepted (p=0.244)	Declined (p=0.043)	Declined (p=0.000)	Accepted (p=0.153)	Accepted (p=0.153)	Accepted (p=0.096)	Accepted (p=0.112)	Declined (p=0.039)

To further investigate the reasons for the declined normality, a Q-Q plot was generated for each material (Figure S7). Upon inspection, the Q-Q plots for Copper, Fiberglass, and Lubricating oil clearly revealed the presence of two distinct outliers. Despite these outliers leading to a decline in normality by the Shapiro-Wilk test, normality was nonetheless accepted for these materials. This decision is justified by the understanding that outliers, while affecting statistical tests, do not always invalidate the underlying distribution, especially when the bulk of the data still aligns with a normal distribution [71]. For practical modeling purposes, and given the identified cause, a normal distribution was deemed sufficiently representative for these materials.

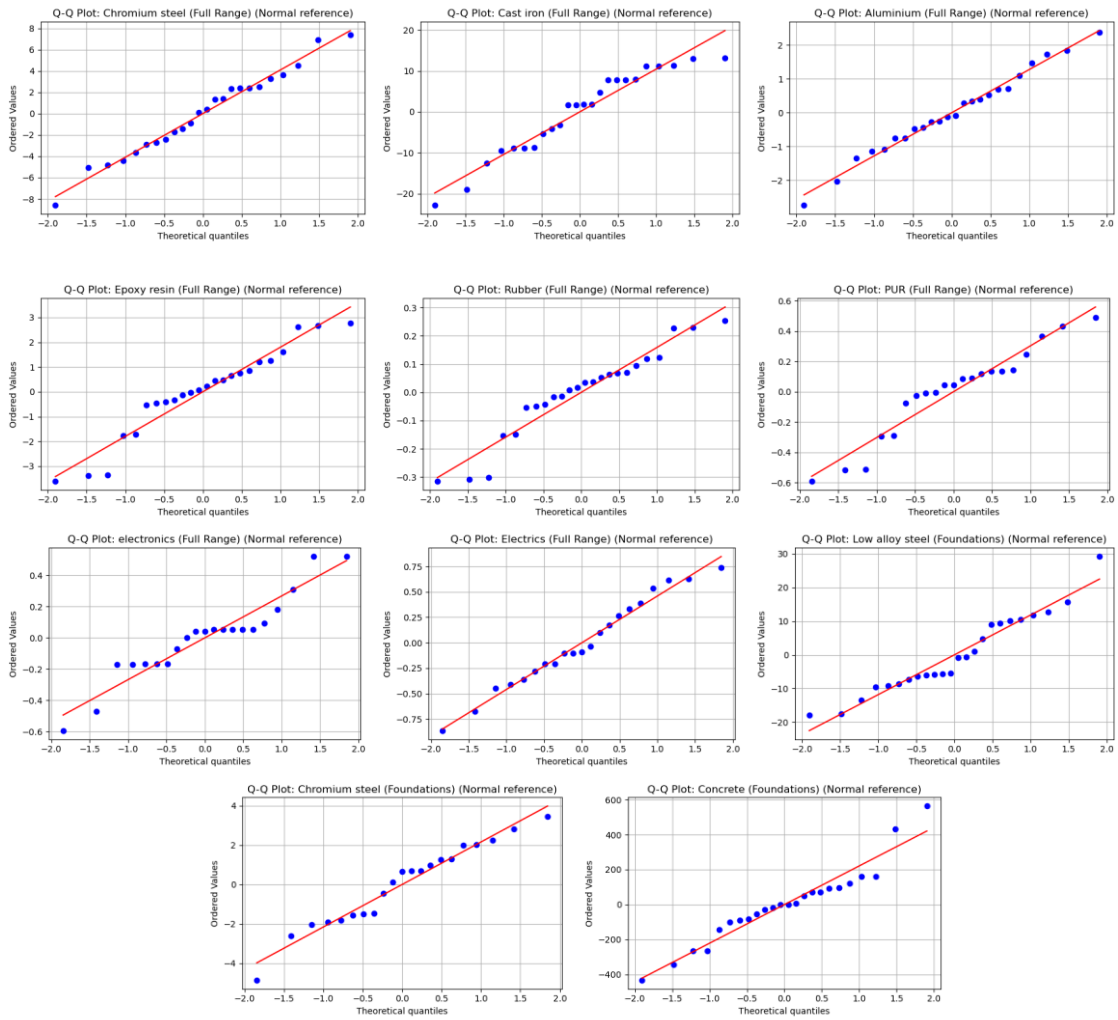

Figure S6. Q-Q plots for all materials for which the Shapiro test was accepted.

Conversely, the Q-Q plot for Low Alloy steel did not exhibit such clear outliers. In this specific case, further investigations into alternative residual distributions were conducted. We sequentially tested for lognormality (using the Shapiro-Wilk test on log-transformed residuals), triangular, and uniform distributions, both latter employing the Kolmogorov-Smirnov test. The lognormality and triangular tests were declined, indicating a poor fit. However, the uniform distribution test yielded an acceptance (p=0.063), suggesting that a uniform distribution provides a more appropriate description for the residuals of Low Alloy steel. Consequently, a uniform distribution was applied for the statistical treatment of Low Alloy steel residuals.

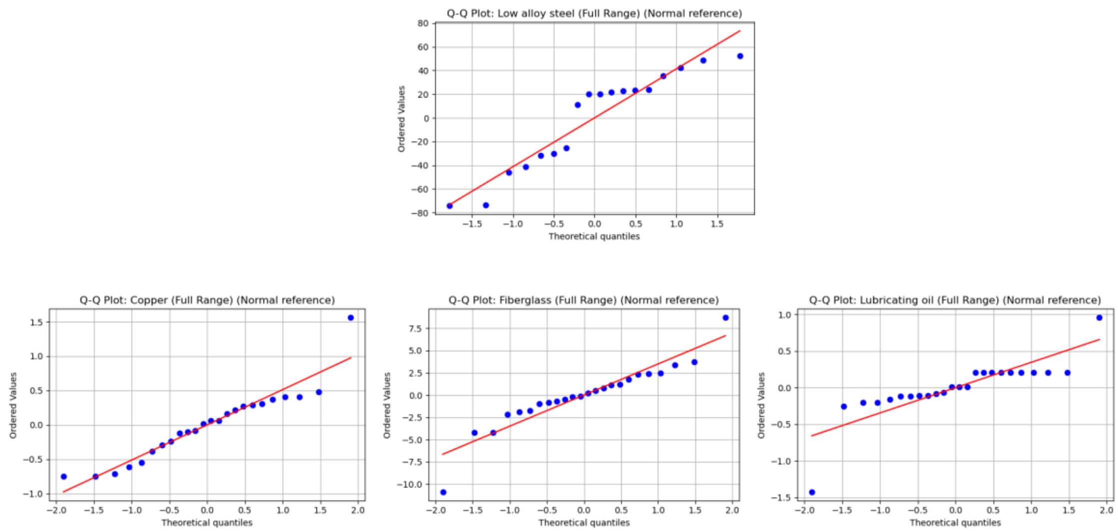

Figure S7. Q-Q plots for all materials for which the Shapiro test was rejected.

1.1.2. Modelling the background of steel

WindTrace assumes that steel is produced in Europe and adapts the inventories. It takes into account annual data on: (1) the share of steel produced in each country (e.g., 27% Germany, 16% Italy, 9% France, 8.4% Spain, …), and (2) the secondary steel share (e.g., 43% secondary, 57% primary). By default, data is taken from the European Steel in Figures Report 2022 [28], which shares data series on the steel production by country from 2017 to 2021 and on secondary steel production from 2012 to 2021.

In Ecoinvent, secondary steel production can be represented by the activity 'steel production, electric, low-alloyed', while primary production can be represented by the activity 'steel production, converter, low-alloyed'. Instead of using these unmodified activities, WindTrace adapts the share and location of all the natural gas and medium voltage electricity inputs for the primary and secondary steel production activities according to Eurofer's data. Although natural gas adaptation would always follow this pathway, the electricity mix can be manually fine-tuned. This is done by changing the input variable 'Electricity mix steel' (electricity_mix in the python package code) to either 'Europe', 'Poland', or 'Norway'. This would take the amount of electricity needed to produce primary and secondary steel and would assign it to the activity 'market for electricity, medium voltage' for the Ecoinvent location of 'RER', 'PL', or 'NO', respectively.

After this, WindTrace considers that the turbine is manufactured one year before the commissioning date (given as an input by the user), and it creates a new market activity considering the share of primary and secondary steel of that year. Eurofer provides time series data on primary and secondary steel shares only for 2012–2021. For turbines manufactured outside this period, WindTrace uses the average share over these years. Since the 2012-2021 series values vary only slightly (from a minimum of 40.6% in 2016 to a maximum of 43.7% in 2018), this simplification has little effect on the results. If the user wants to use another secondary share (not following Eurofer's data), this is possible by manually changing the input variable 'Recycled steel share' (recycled_share in the python package code) by the desired share.

Applying the background changes with Eurofer's data, the modelled Climate Change impact (ReCiPe 2016 v1.1 midpoint (H)) in the period 2012-2021 oscillates between 1.499 and 1.546 kg CO_{2eq} per kg of steel produced. This variability is very small, as the share of secondary production steel does not change much with time either, oscillating between 40.5% and 43.5%. However, there is 25% of impact reduction if these values are compared to the Climate Change intensity of Ecoinvent's global market (transportation discounted). This is the result of allocating production in Europe, with a lower carbon intense electricity mix compared to the World average.

1.2. Modelling the manufacturing and transport phases

Table S6 summarises the turbine and foundations manufacturing processes and the Ecoinvent background processes in WindTrace.

Table S6. Summary of the manufacturing processes included in the LCI and the chosen Ecoinvent activity.

Material	**Part (Turbine or Foundations)**	**Manufacturing process (Ecoinvent v3.9.1 activity)**
Copper	Turbine	market for wire drawing, copper**
Aluminium	Turbine	market for sheet rolling, aluminium
Chromium steel	Turbine/Foundations	market for sheet rolling, chromium steel
Steel	Turbine/Foundations	market for section bar rolling, steel
	Turbine	market for welding, arc, steel
Cast iron	Turbine	market for section bar rolling, steel**
Zinc*	Turbine	zinc coating, pieces

*Zinc is a coating used for protection in the tower. The process 'zinc coating, pieces' already contains the amount of zinc required for the coating. Thus, zinc has not been included as a material input to avoid double accounting.

**'market for wire drawing, copper' is a proxy both for aluminium wire drawing and copper sheet rolling in the turbine, because a better fitting activity does not exist in Ecoinvent. Same with 'market for section bar rolling, steel' for cast iron in the turbine.

All the material processing activities have a functional unit of kilograms except for 'market for welding, arc, steel', which is in meters. In this case, two times the hub height was defined as the amount of the process, following Sacchi et al. [41]. The electronics and electric components (i.e., cables) inside the turbine have not been assigned processing activities because they are already included in the materials dataset selected in the material's phase.

The transportation phase includes the delivery of the materials from the manufacturing site to the wind park location. We assume a single manufacturing site for all wind turbine parts except for the tower and the foundations. The closest manufacturing facility of the manufacturer is chosen, and road transportation in a straight-line distance is assumed. As the tower (steel) and foundations (concrete) are usually manufactured in a different manufacturing site, not owned by the same company, we assume 450 km truck transportation of steel and 50 km truck transportation of concrete, following Vestas' reports (see Vestas, (2018b) as an example).

1.3. Modelling the installation phase

1.3.1. Modelling the foreground

According to Denholm et al. [29], the land use changes in a wind park can be divided into permanent (i.e., those that will last the entire lifetime of the wind park) and temporary (i.e., those that happen during the installation and that will recover its previous state in a few years even while the turbine is still operating).

First, WindTrace considers the total area of permanent and temporary changes. By default, it takes intensities of 3000 m^2/MW and 7000 m^2/MW, respectively. These values are derived at the wind farm level, i.e., they represent average land-use intensities per unit of installed capacity, based on 172 wind park projects in the US commissioned between 2000 and 2009, with an average turbine capacity of 1.6 MW [29]. In our model, we allocate these farm-level intensities to individual turbines on a per-MW basis. However, the permanent value can be manually adapted by changing the input parameter 'Land use permanent intensity' (land_use_permanent_intensity in the Python code). Then, transformation and occupation flows are calculated considering the type of land cover prior to the wind park installation. The land cover type can be assigned as a parameter. However, if the user has no information, it is assigned according to the probability of occurrence of each land cover type in Siemens Gamesa [30], which is based on data on land cover types of European wind farms.

Transformation flows describe from which initial to which final type of land cover the land use is being transformed. Initial land cover types, and associated biosphere transformation flows are described in Table S7**Error! No s'ha trobat l'origen de la referència.**.

On the other hand, the final type of land cover depends on the use that the land is given when the wind park is installed. In this case, the biosphere flow "Transformation, to traffic area, road network" was chosen when the final land purpose was related to roads, and "Transformation, to industrial area" for the rest of purposes (Table S8).

Table S7. Land cover typology prior to the installation of a wind farm, their probability of occurrence, and biosphere flows selected to model the transformation in WindTrace. Data from Siemens Gamesa [30] based on European wind parks.

Land cover type	**Share of projects installed on this land cover**	**Biosphere 3 'Transformation' flow**
Forest	30.6%	Transformation, from forest, unspecified
Non-irrigated crops	21.0%	Transformation, from annual crop, non-irrigated
Row crops	11.5%	Transformation, from annual crop
Shrubland	17.4%	Transformation, from shrub land, sclerophyllous
Pasture	7.9%	Transformation, from pasture, man made
Unspecified	7.2%	Transformation, from unspecified
Industrial	4.4%	Transformation, from industrial area

Table S8. Permanent and temporary area coverage per type of area. Data reproduced from Denholm et al. [29].

Permanent impacts		**Temporary impacts**	
Wind park areas	**Area coverage**	**Wind park areas**	**Area coverage**
Roads	79%	Temporal roads	62%
Turbine	10%	Staging area	30%
Substation	6%	Substation construction	6%
Transformer	2%	Other	3%
Others	2%		
Intensity	3000 m^2/MW	**Intensity**	7000 m^2/MW

Occupation flows (Ecoinvent nomenclature) consider for how long that area is being occupied by the new land use. In this case, the "Occupation, traffic area, road network" and "Occupation, industrial area" where chosen for network and all other purposes, respectively. For permanent impacts, we considered the lifetime of the turbine, while for the temporary impacts, we assumed the area was completely restored in 2.5 years. This process is summarised in Equations S1-S5.

Equation S1. Transformation, from land cover type (m2) = (3000 + 7000) (m2/MW) * turbine power (MW)

Equation S2. Transformation, to industrial area (m2) = 7000 (m2/MW) * 0.21 * turbine power (MW) + 7000 (m2/MW) * 0.21 * turbine power (MW)

Equation S3. Transformation, to traffic area, road network (m2) = 7000 (m2/MW) * 0.79 * turbine power (MW) + 7000 (m2/MW) * 0.79 * turbine power (MW)

Equation S4. Occupation, industrial area (m2*year) = 3000 (m2/MW) * 0.21 * turbine power (MW) * lifetime (years) + 7000 (m2/MW) * 0.21 * turbine power (MW) * 2.5 (years)

Equation S5. Occupation, traffic area, road network (m2*year) = 3000 (m2/MW) * 0.79 * turbine power (MW) * lifetime (years) + 7000 (m2/MW) * 0.79 * turbine power (MW) * 2.5 (years)

1.3.2. Modelling the road background

For the road construction, gravel-based roads without asphalt were assumed. The original Ecoinvent activity 'road construction' was adjusted, removing asphalt-related inputs and wastes. Moreover, land use was also removed from the activity to avoid double accounting. Thus, the activity includes gravel as a material, and diesel and electricity for the excavation process as transforming activities. Only permanent roads construction was considered, while temporary roads were left out of the scope due to lack of data on their composition.

To calculate the length of the roads installed, a surface road network intensity of 2370 m^2/MW was used as indicated in Table S8, and a width of 5 m was considered [31].

Finally, the excavation activities were modelled according to the volume of the foundation materials.

1.4. Modelling the end-of-life phase

We use the cut-off approach to model the end-of-life phase in WindTrace. Figure S8 illustrates this approach with steel as an example, showing its role both before turbine construction (left) and at the end-of-life stage (right). In WindTrace, steel demand is represented as a mix of primary and secondary steel. To capture this, we developed a region-specific European market model (taged as NEW activity in the Figure) based on Eurofer data (2012–2021), which reflects historical shares of primary and secondary production. These data show that Europe has a lower share of primary steel production (56.4–59.5%) compared to the global average (74%), a difference that substantially affects environmental impacts given the large steel requirements of wind turbines.

Within the cut-off approach, recycled materials enter the system burden-free, thereby encouraging their use in the input mix. For instance, in the Figure, iron scrap, the main input to secondary steel production, enters the system without upstream burdens. However, the recycling process required to transform scrap into usable steel is fully accounted for. By contrast, virgin iron used in primary steel production carries the full burdens of extraction and processing.

At the end-of-life stage, we assign recycling shares to each material according to three scenarios described later in this section. In two of these scenarios, we assume that 90% of steel is recycled. Under the cut-off approach, this recycled share exits the system without burdens or credits, while the remaining 10% is sent to landfill, where the associated disposal impacts are included in the system boundary.

Three scenarios can be chosen for the end-of-life: the standard (std), optimistic (op) and pessimistic (ps). The standard was defined following Bang et al. [32] and is the one used by default in WindTrace and applied to all assessments in this study. The pessimistic scenario was adapted from Li et al. [33]. We also propose an optimistic scenario based on four assumptions:

1. Rare earth metals are easier to recover, especially from permanent magnets in the permanent magnet direct driven generators, which have high recycling potential [34].
2. Fibreglass and epoxy resin from current blades can be recycled. This assumption is based on the many chemical and thermal treatments already under investigation [35].
3. Electronics are mostly recycled.

4. Concrete aggregates are recycled as it is already the case in several applications [36].

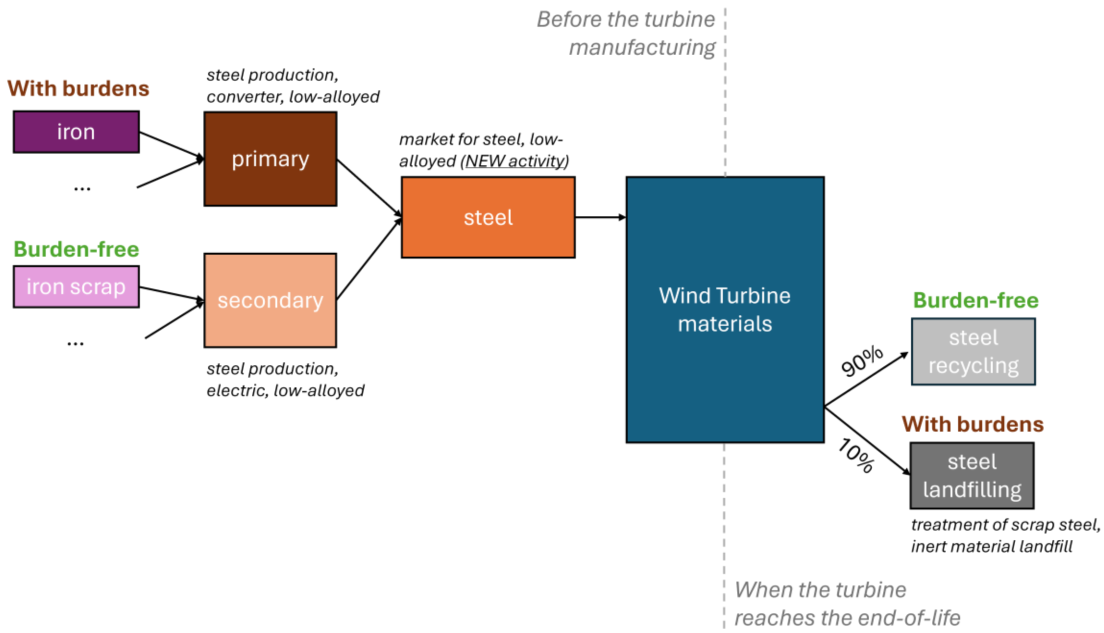

Figure S8. Schematic representation of end-of-life modelling in WindTrace, illustrated with steel as an example. Names of Ecoinvent activities used in itallics.

The recycling, landfill and incineration rates of all materials and scenarios are listed in

Table S9. Ecoinvent activities selected for incineration and landfilling are described in

Table S10. No activities for recycling were chosen.

We assume that no components of the wind turbine are reused following the end of its operational life. Additionally, we do not account for the replacement of any components during the turbine's lifetime. As a result, all components are considered to have the same lifetime as the turbine itself, which is specified manually as a user-defined input within the model. Consequently, all materials physically embedded in the turbine are assumed to reach their end of life simultaneously and are subsequently directed to one of three end-of-life treatment pathways as described in Table S9: recycling, landfilling, or incineration.

Table S9. End-of-life scenarios defined in WindTrace.

	End-of-life scenarios (% of weight)								
	Standard (std)			Optimistic (op)			Pessimistic (ps)		
Material	Recycling	Landfill	Incineration	Recycling	Landfill	Incineration	Recycling	Landfill	Incineration
Iron and alloys	90	10		90	10		52	48	
Copper	90	10		90	10		42	58	
Aluminium	90	10		90	10		42	58	
Rare earth metals		100		70	30		1	99	
Plastics			100			100			100
Fibreglass and resins			100	70		30			100
Lubricants			100			100			100
Electrics and electronics		100		50	50			100	
Concrete		100		50	50			100	

1.5. Modelling the wind park

1.5.1. Modelling the cables

Intra-array cables connecting the turbines among them were modelled assuming 33kV 3-core cables buried underground. The modelling included the materials, manufacturing and excavation activities for the installation. The materials were modelled with data from Nexans' cable technical datasheet [37] consisting of a conductor (copper/aluminium), and insulator (polyethylene; PE) and an outer sheath (polyvinyl chloride; PVC), as shown in

Table S11**Error! No s'ha trobat l'origen de la referència.**. Because according to Vestas' reports, both aluminum and copper are used for the intra-array cables indistinctively, the modelling considers an arbitrary even material distribution of 50% each.

The section of the cables was calculated as a function of the park power, retrieving from a second order regression curve. A distance between turbines of 8-12 times the rotor diameter (D) headwind and 4-6D crosswind is recommended in the literature [38,39]. For simplicity, a single headwind array of 8D is applied in the model. The mass of the conductors (copper and aluminium) was calculated like in Equation S6. Other materials' masses were rescaled according to their mass share in the cable.

Equation S6. Conductor mass (kg) = cable section (m^2) * 8D (m) * (number of turbines – 1) * conductor's density (kg/m^3)

Table S10. Ecoinvent activities to model the end-of-life of the materials in the turbine and foundations.

Material	Ecoinvent 3.9.1 activity	Is proxy
Low alloy steel	treatment of scrap steel, inert material landfill	No
	treatment of scrap steel, inert material landfill	No
Chromium steel	treatment of scrap steel, inert material landfill	Yes
Cast iron	treatment of scrap steel, inert material landfill	Yes
Aluminium	treatment of waste aluminium, sanitary landfill	No
Copper	treatment of copper slag, residual material landfill	No
Rare earth metals	treatment of inert waste, sanitary landfill	Yes
Epoxy resin	treatment of inert waste, sanitary landfill	Yes
Rubber	treatment of inert waste, sanitary landfill	Yes
PUR	treatment of inert waste, sanitary landfill	Yes
PVC	treatment of waste polyvinylchloride, sanitary landfill	No
Fibreglass	treatment of waste glass, sanitary landfill	Yes
Electronics	treatment of inert waste, sanitary landfill	Yes
Electrics	treatment of inert waste, sanitary landfill	Yes
Lubrication oil	treatment of waste mineral oil, hazardous waste incineration, with energy recovery	No
Concrete	treatment of waste concrete, inert material landfill	No

Table S11. Summary of the materials and their shares in the LCI of the wind park intra-array cables and the Ecoinvent activities for the material and the manufacturing process.

Material in WindTrace	Material Ecoinvent v3.9.1 activity	Manufacturing Ecoinvent v3.9.1 activity	Share of material in the cable (%)
Aluminium	market for aluminium, wrought alloy	market for wire drawing, copper	61
Copper	market for copper, cathode	market for wire drawing, copper	
Polyvinyl chloride (PVC)	market for polyvinylchloride, bulk polymerised	extrusion, plastic film	9
Polyethylene (PE)	polyethylene, high density, granulate	extrusion, plastic film	30

1.5.2. Modelling the transformer

The turbines are connected to a transformer prior to the connection to the grid. This transformer is included in the system boundaries of the wind park. In WindTrace, the transformer is modelled according to data on material intensities from the Environmental

Product Declaration of a power transformer TrafoStar 500 MVA from ABB (2000). The adaptation of this inventory to Ecoinvent was made following Sacchi et al. [41]. However, in the case of WindTrace, the transformer is scaled to the power of the park, considering an equivalence of 1:1 between MVA and MW.

2. WindTrace validation

2.1. Materials phase Montecarlo analysis

Section 3.2 in the main text presents a contribution analysis of environmental impacts per life-cycle stage (materials, manufacturing, transport, installation, maintenance, and end-of-life) of the Vestas V80/2.0 modelled with WindTrace. Results show that the materials phase is the most impactful. The contribution of this phase is 83.6% for Climate Change and between 73.2% and 96.9% for the rest of impact categories except for land occupation, which depends on the installation.

Moreover, the material composition of a wind turbine depends on its design, even among turbines with the same power. For example, the aluminium mass of all 2 MW Vestas turbines can vary up to 141% depending on the turbine design (Figure S1). Due to the lack of alternative data sources, data used in WindTrace only comes from one manufacturer (i.e., Vestas). Therefore, it is crucial to assess the uncertainty of the materials life cycle stage.

Table S12. Difference in % between the static LCIA value and the upper and lower 95% confidence interval values for ReCiPe 2016 v1.1 midpoint (H) impact categories. Terrestrial Acidification (TA), Climate Change (CC), Freshwater Ecotoxicity (FET), Marine Ecotoxicity (MET), Terrestrial Ecotoxicity (TET), Fossil Resource Scarcity (FRS), Freshwater Eutrophication (FE), Marine Eutrophication (ME), Human Toxicity: Cancer (HTc), Human Toxicity: Non-cancer (HTnc), Ionising Radiation (IR), Land Use (LU), Mineral Resource Scarcity (MRS), Ozone Depletion (OD), Fine Particulate Matter Formation (PMF), Photochemical Oxidant Formation: Human Health (HOF), Photochemical Oxidant Formation: Ecosystems Quality (EOF), Water Use (WU).

	Impact category																	
	TA	CC	FET	MET	TET	FRS	FE	ME	HTc	HTnc	IR	LU	MRS	OD	PMF	HOF	EOF	WU
Lower	-17.6	-13.7	-147.0	-129.2	-48.6	-14.6	-95.8	-28.1	-69.8	-2374.6	-220.6	-6.8	-19.9	-35.2	-18.4	-22.7	-22.6	-23.8
Upper	60.2	39.3	23.6	26.6	147.7	49.6	103.0	45.1	122.1	2373.4	352.9	14.4	33.7	92.8	67.9	79.3	83.1	43.9

With this purpose, we carried out a Montecarlo analysis consisting of 1200 LCIA runs of the Reference Turbine. In 11 impact categories, the difference between the static LCIA result and the upper or lower confidence interval is smaller than 100%, while in 5 impact categories, one of the differences is between 100% and 150% (Table S12). Finally, HTc and IR are the categories with higher uncertainties, with differences between 221-353% and 2375-2373%, respectively. Histograms of the Montecarlo analysis are shown in Figure S9.

2.2. Validation with Vestas reports original data

As the Montecarlo analysis concludes that uncertainties in the material stage are not negligible, a validation of WindTrace's inventories is required to ensure the reliability of the results.

- LCI Validation

We analysed the materials LCIs results of 18 Vestas original datasets and contrasted them with the materials LCIs of the same turbines modelled using WindTrace. The mean deviations range from 7.23% (chromium steel) to 18.05% (copper) (Table S13). However, lubricating oil and chromium steel (foundations) are out of this range. In the first case, because it has two clear outliers in the input data (see 6.0MW and 6.2MW turbines in Figure S1). For chromium steel (foundations), the fitting curve is very poor (Figure S1).

- LCIA Validation

We carried out the same analysis as in Section S1.1.1.1, analysing the LCIA results of 18 Vestas original datasets and contrasting them with the LCIA results of inventories modelled using WindTrace. We applied Mean Squared Error (RMSE), Mean Percentage Error (MPE), and R^2 for the comparison. Given the strong influence of the steel and foundations in the total mass of the turbine, the process was repeated with and without.

Overall, the modelled LCIA impacts show a R^2 value between 0.92 and 0.97 and a RMSE between 5% and 9% of the mean predicted value in the analyses with steel and foundations (Table S14, Figure S5, Figure S10).

Table S13. Mean of the absolute variation of each materials comparing Vestas original data with WindTrace modelled materials.

Material	Steel	Chromium steel	Iron	Aluminium	Copper	Epoxy resin	Rubber	PUR
Mean ± SD (%)	16.0 ± 15.1	7.2 ± 5.6	14.6 ± 8.6	15.8 ± 9.3	18.1 ± 13.1	11.3 ± 10.5	11.6 ± 10	11.1 ± 11.5

Material	PVC	Fibreglass	Electronics	Electrics	Lubricating oil	Steel (foundations)	Chromium Steel (foundations)	Concrete (foundations)
Mean ± SD (%)	11.1 ± 11.5	8.5 ± 6.7	17.9 ± 14.7	13.5 ± 9.9	30.5 ± 62.7	13.5 ± 8.2	116.2 ± 219.4	15.4 ± 13.1

Similarly, the results without steel and foundations show R^2 between 0.90 and 0.97 and RMSE between 5% and 9%. Although in the analysis with steel and foundations the model tends to slightly overestimate the results with positive values between 0.25% and 6.31%, a general trend of slight underestimation is observed in the analysis without steel and foundations, with 12/18 impact categories with negative values between -0.09% and -0.32%. The categories with higher MPE are OD, WU, and ME, where there is a small overestimation of impacts, especially for small turbines. This is because WindTrace slightly overestimates the mass of fibreglass for small turbines, being fibreglass the top contributor to these three impact categories. Although the results show a good material mass predicting behaviour by WindTrace, a limitation is that we are using a subset of Vestas' datasets to do the validation and also to feed the material stage modelling in WindTrace. However, lack of other data availability does not allow to have a separated wind turbine validation dataset.

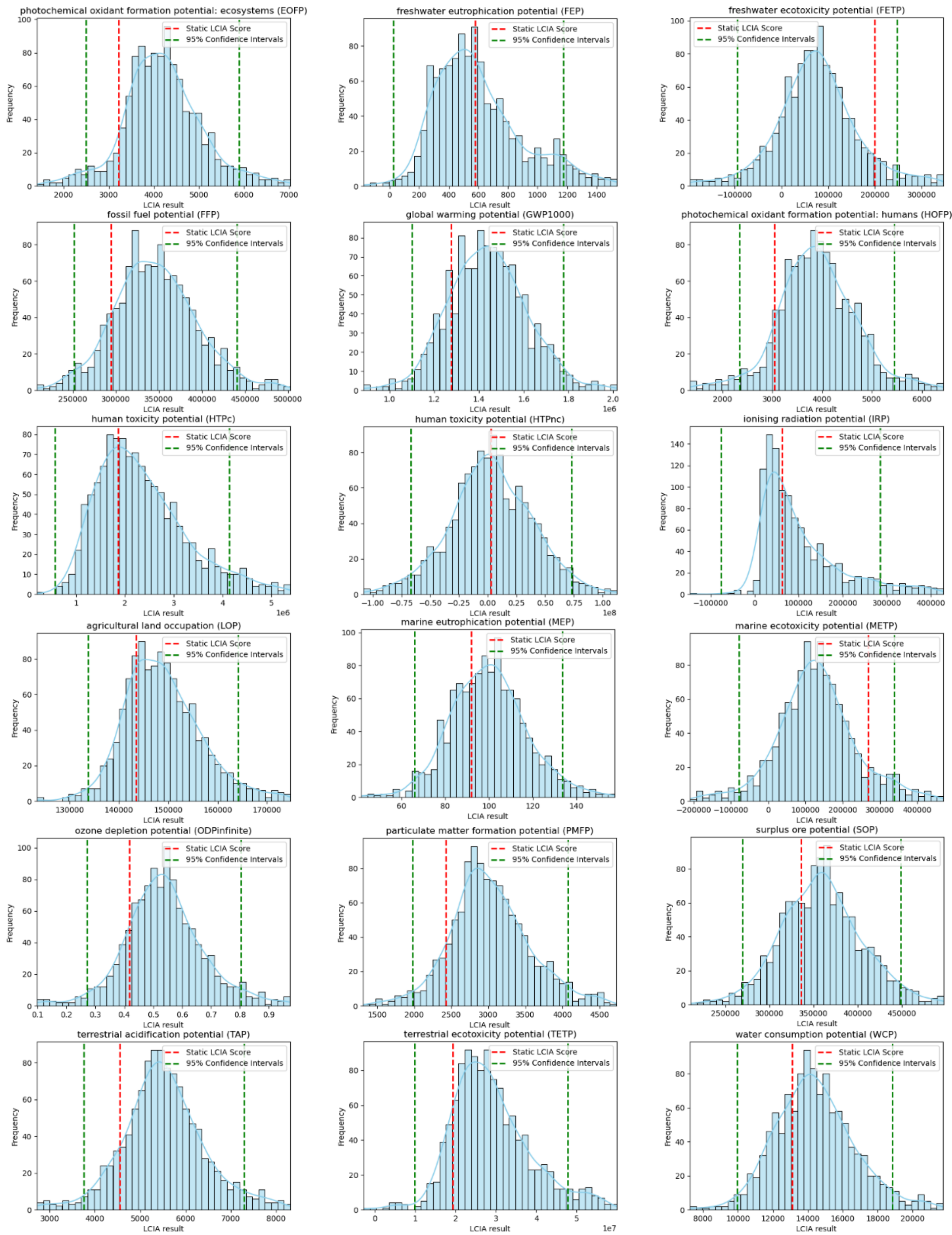

Figure S9. Montecarlo LCIA analysis of 1200 runs for all methods in ReCiPe 2016 v1.1 midpoint (H).

Table S14. LCIA results comparison of WindTrace modelled Vestas' turbines and the LCIA results from the original masses reported by Vestas. Both LCIA results are given with and without steel and foundations.

	With steel and foundations			Without steel and foundations		
Impact category	**R^2**	**RMSE (%)**	**MPE (%)**	**R^2**	**RMSE (%)**	**MPE (%)**
Climate Change (CC)	0.96	6	1.55	0.97	5	1.11
Ozone Depletion (OD)	0.95	6	4.73	0.94	8	5.57
Ionising Radiation (IR)	0.96	6	0.84	0.97	5	-0.65
Fine Particulate Matter Formation (PMF)	0.97	5	0.35	0.97	5	-0.66
Photochemical Oxidant Formation: Ecosystem Quality (EOF)	0.96	6	0.89	0.97	5	-0.13
Photochemical Oxidant Formation: Human Health (HOF)	0.96	6	0.89	0.97	5	-0.10
Terrestrial Acidification (TA)	0.97	5	0.92	0.97	6	0.41
Freshwater Eutrophication (FE)	0.97	6	0.17	0.95	7	-1.23
Marine Eutrophication (ME)	0.93	8	6.31	0.90	9	7.52
Human Toxicity: Cancer (HTc)	0.92	9	0.68	0.91	9	-3.14
Human Toxicity: Non-cancer (HTnc)	0.95	7	0.25	0.93	9	-0.11
Terrestrial Ecotoxicity (TET)	0.96	6	-0.05	0.96	7	-0.47
Freshwater Ecotoxicity (FET)	0.95	7	0.39	0.93	9	-0.09
Marine Ecotoxicity (MET)	0.96	7	0.36	0.93	9	-0.17
Land Use (LU)	0.96	6	0.28	0.97	5	-1.06
Water Use (WU)	0.96	6	4.55	0.94	8	5.62
Mineral Resource Scarcity (MRS)	0.92	10	0.72	0.91	9	-3.32
Fossil Resource Scarcity (FRS)	0.97	6	1.80	0.97	5	1.56

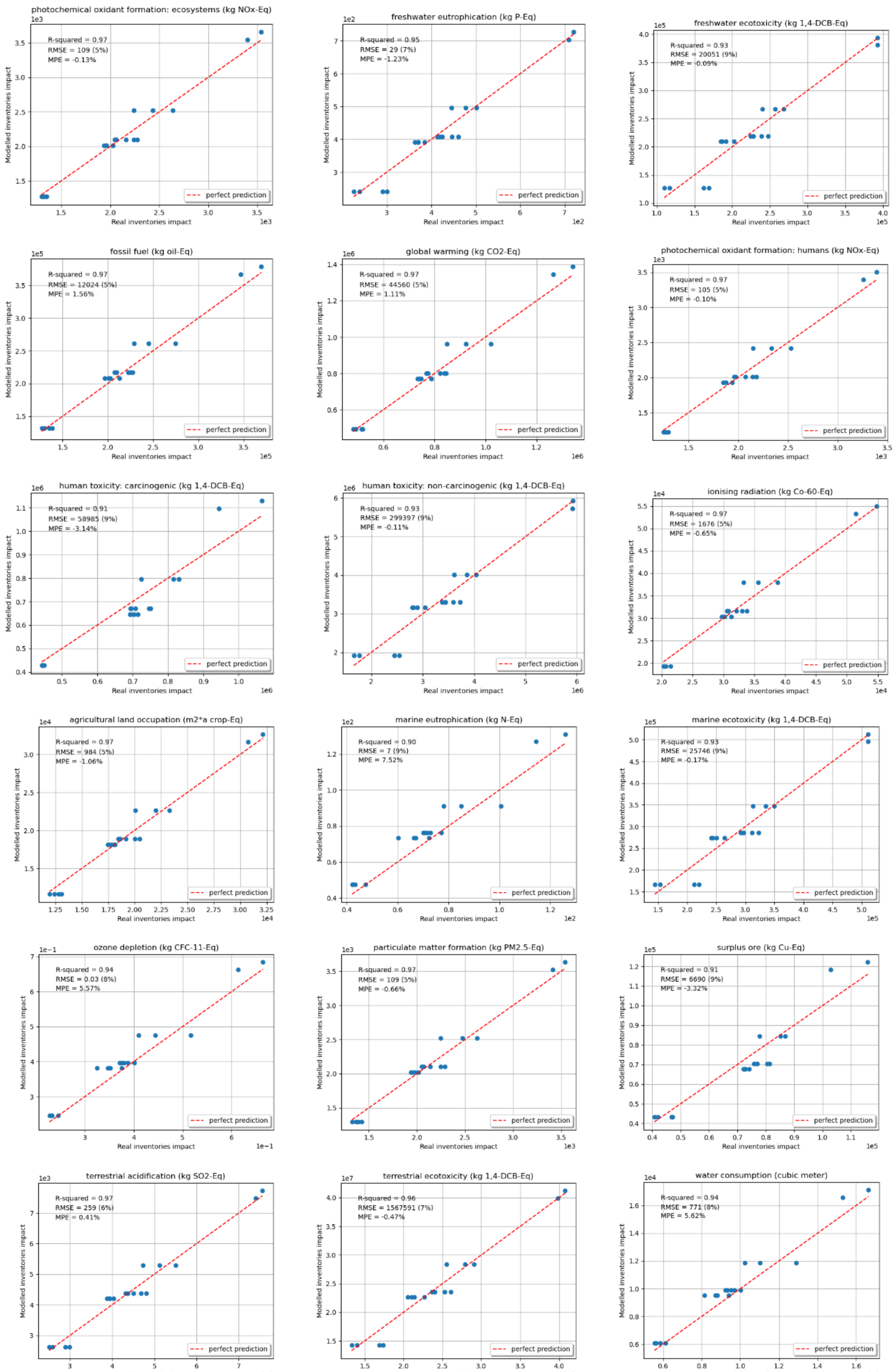

Figure S10. LCIA results comparison between the inventories modelled with WindTrace and the inventories using original data from Vestas reports (without steel and foundations).

3. Comparison of WindTrace and Ecoinvent

3.1. Methods and Limitations

To analyse the case studies, we define a Reference Turbine based on the Vestas V90/2.0, the most installed onshore turbine in Europe up to 2021 (Pierrot, 2021). The parameters defining the Reference Turbine are detailed in Table S15, which also illustrates how this Reference is modified in the two case studies by adjusting specific parameters. A contribution analysis of Ecoinvent's 800 kW (N50/800), 2 MW (Vestas V80/2.0) and 4.5 MW (Enercon E-112) was carried out and compared to WindTrace.

A potential concern in our analysis is the issue of data circularity, given that one of the data points used in the WindTrace model (the 800 kW turbine) is also included in the comparison with Ecoinvent data presented in this section. Specifically, the WindTrace regression dataset includes information for an 800 kW turbine, and we also compare WindTrace outputs against Ecoinvent's datasets for 800 kW (Nordex N50/800), 2 MW (Vestas V80/2.0), and 4.5 MW (Enercon E-112) turbines, all of which are derived from Burger & Bauer (2007).

Despite this overlap, we consider the comparison in the 0–1 MW range (Figure 2a in the main text) to be methodologically sound for three main reasons:

- Steel mass regression excludes Burger & Bauer data:

Steel mass is the dominant contributor to the environmental impacts of wind turbines (e.g., contributing 36.2% of Climate Change impacts for the 2 MW turbine, see Table S15). In the WindTrace model, steel mass is regressed as a function of hub height. Because the Burger & Bauer study does not report hub height for the 800 kW turbine, this data point was excluded from the steel mass regression. As a result, the most impactful parameter in the model is not influenced by the 800 kW Ecoinvent data, mitigating concerns of circularity.

- Other material masses are derived from global regressions:

While the 800 kW turbine is included in the WindTrace dataset, the mass of other materials (e.g., concrete, fiberglass) is determined through regression across the entire dataset and not solely based on the 800 kW data point. Therefore, material masses in the WindTrace-modeled 800 kW turbine are not directly reflective of Burger & Bauer values.

- Divergence in life-cycle stage modelling approaches

Beyond material production, the modelling logic used in WindTrace differs significantly from that of Burger & Bauer. For example, WindTrace employs updated assumptions for transportation, end-of-life treatment, and installation logistics, ensuring that life-cycle stage contributions differ even when similar capacity values are compared.

3.2. Comparison Results

Unlike WindTrace, Ecoinvent's inventories are not classified in LCA phases (i.e., materials, manufacturing, transport, installation, maintenance, and end-of-life). Thus, we had to manually classify the inventory flows. Inputs identified as materials were assigned to the materials phase, while their industrial processes were assigned to the manufacturing phase. Installation included land use flows and excavation activities. Wastes were classified as end-of-life and no transportation activities were identified. Maintenance was taken from the activity 'electricity production, wind, 1-3MW turbine, onshore' in Germany and rescaled.

The results of the comparison are shown in Figure S11. Minimal differences are observed among modelled contribution analysis (only marginal decrease in installation for Land Use in 800 kW, and marginal increase in materials for SO in 4.5 MW because it has proportionally more rare earth, as the generator is dd_eesg instead of gb_dfig). The only significant difference comes when comparing the Land Use indicator, where in Ecoinvent's 4.5MW the installation is only 28% instead of around 80% as in any of the other turbine powers and the modelled 4.5MW. The explanation is two-fold: first, the land use intensity is 69.8 m^2/MW, versus 1400 m^2/MW in 800kW or 112.5 m2/MW in 2MW. Second, in the materials phase the amount of copper for the 4.5MW is 20 times the amount in the 2MW turbines. Because copper is the highest material input in terms of LOP/kg (1.113 m^{2*}a crop-Eq, in front of 0.031 m^{2*}a crop-Eq in cast iron, or 0.043 m^{2*}a crop-Eq in steel, for example), the direct land use impact during the deployment of the turbine is reduced, due to the land use intensity in the background for copper mining. Moreover, although 800 kW does not include excavation activities, this does not affect much the contribution of the installation phase.

Table S15. Reference Turbine parameters, and parameter changes introduced in each section in the main text. In blue, Ecoinvent or unapplicable parameters. In purple, parameter variations in WindTrace. In orange, constant values for the Reference Turbine. In all sections, the park power was 2.0 MW and the number of turbines was one.

		3. Comparison of WindTrace and Ecoinvent				4.2 Understanding the influence of sensitive parameters to the environmental impacts of wind turbines using WindTrace (FU: MW)			4.3 Understanding the influence of sensitive parameters to the environmental impacts of wind turbines using WindTrace (FU: kWh)	
		3.3		3.2		4.2.1	4.2.2	4.2.3	4.3.1	4.3.2
		Contribution analysis		Impact comparison		Power	Steel production	Generator	Lifetime	Capacity factor
Parameter	**Reference Turbine**	**Ecoinvent**	**WindTrace**	**Ecoinvent**	**WindTrace**	**WindTrace**	**WindTrace**	**WindTrace**	**WindTrace**	**WindTrace**
Park location	DE	-	DE	-	DE	DE	DE	DE	DE	DE
Park coordinates (latitude, longitude)	(53.4356, 11.2142)	-	(53.4356, 11.2142)	-	(53.4356, 11.2142)	(53.4356, 11.2142)	(53.4356, 11.2142)	(53.4356, 11.2142)	(53.4356, 11.2142)	(53.4356, 11.2142)
Manufacturer	Vestas	Vestas	Vestas	**Nordex, Vestas, Enercon**	Vestas	Vestas	Vestas	Vestas	Vestas	Vestas
Rotor diameter (m)	90	**80**	**80**	**50, 80, 113**	90	90	90	90	90	**50, 90, 113**
Turbine power (MW)	2.0	2.0	2.0	**0.8, 2.0, 4.5**	**0.0 - 5.0**	**0.0 - 10.0**	2.0	2.0	2.0	**0.8, 2.0, 4.5**
Hub height (m)	97.14	**78**	**78**	**Unknown, 78, 120**	**40, 80, 120**	**40, 60, 80, 100, 120, 140**	97.14	97.14	97.14	**50.6, 97.14, 120**
Commissioning year	2011	-	2011	-	2011	2011	2011	2011	2011	2011
Recycled steel share	0.416	**0.258**	0.416	**0.258**	0.416	0.416	**0 - 1**	0.416	0.416	0.416
Electricity mix steel	European Union (EU) [2022]	-	EU (2022)	-	EU (2022)	EU (2022)	**Norway, Poland, EU (2022)**	EU (2022)	EU (2022)	EU (2022)
Generator type	gb_dfig	gb_dfig	gb_dfig	**gb_dfig, gb_dfig, dd_eesg**	gb_dfig	gb_dfig	gb_dfig	**gb_dfig, dd_eesg, dd_pmsg, gb_pmsg**	gb_dfig	gb_dfig
Land use permanent intensity (m^2/MW)	3000	**112.5**	3000	**1400, 112.5, 69.8**	3000	3000	3000	3000	3000	3000
Land cover type	Row crops	**Pasture**	**Pasture**	**Pasture**	**Pasture**	Row crops	Row crops	Row crops	Row crops	Pasture
End-of-life scenario	Baseline	-	Baseline	-	Baseline	Baseline	Baseline	Baseline	Baseline	Baseline
Lifetime (years)	20	20	20	20	20	20	20	20	**8y - 30y**	20
Capacity factor	0.24	-	-	-	-	-	-	-	0.24	**0.08 - 0.4**
Attrition rate	0.009	-	-	-	-	-	-	-	**0.0, 0.009, 0.02**	0.009

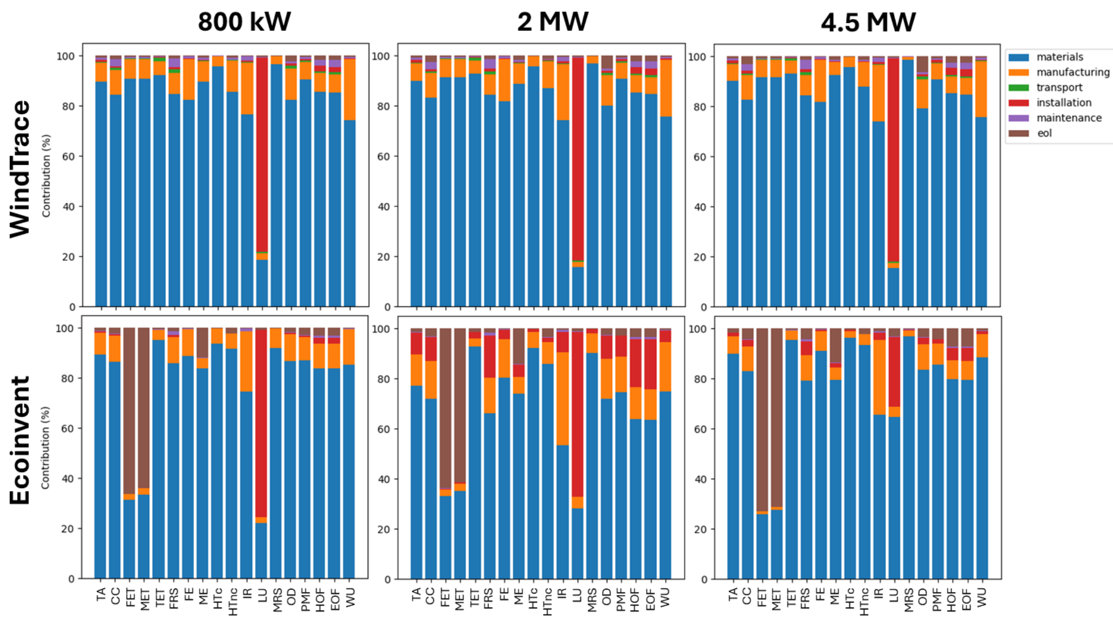

Figure S11. LCIA contribution analysis of 800 kW, 2MW and 4.5 MW turbines from (1) Ecoinvent, and (2) modelled using WindTrace.

We also analyse how much each material contributes to the different impact categories both in the case of WindTrace (Table S16; Figure S12) and Ecoinvent (

Table S17; Figure S13). In WindTrace's analysis steel is the top contributor for all impact categories except FET, HTn, and TET, where copper lead, and ME, OD and WC, where fibreglass dominates impacts. In the case of Ecoinvent, steel is also the top contributor in most impact categories, only surpassed by copper in FET, HTn, MET and TET, and fibreglass in OD.

Table S16. Contribution of each material (in %) to the total impacts of a 2 MW turbine modelled with WindTrace.

	CC	EOF	FE	FET	FF	HOF	HT	HTn	IR	LO	ME	MET	OD	PMF	SO	TA	TET	WC
Steel	36.2	36	38.1	26	34	35.5	71.8	18.7	42.5	4.3	14.8	27.4	17.3	31.9	44.2	26.6	14.6	24.1
Copper	0.9	3.4	12.3	29.6	1	3.5	0.3	29.9	1.5	0.8	1.4	28.4	3.2	8.9	0.9	14.7	28.4	1.7
Chromium steel	12.5	12.2	8.6	6.3	11.8	12.4	13.5	6.7	12.3	2.3	5.7	6.9	9	21.9	4.6	12.3	24.5	6.9
Fibreglass	13.2	9.4	2.2	0.7	17	9.6	0.2	1	6.5	0.6	37.5	0.7	35.7	7	0.1	10.3	0.5	28.8
Concrete	7.8	8.7	2	1	5.1	9	0.2	1.7	1.9	1.2	1.6	1	2.9	3.8	0.3	4.7	2	1.8
Iron	5	5.6	4	1.8	5.3	5.5	9	1.9	2.9	0.5	2.1	2	2.3	4.7	6.4	3.7	1.8	2.1
Electrics	0.7	2.3	7.9	18.8	0.9	2.4	0.2	18.9	1.1	0.5	0.9	18	2.1	5.7	0.5	9.4	18	1.2
Neodymium	0.1	0.1	0.1	0.1	0.1	0.1	0	0.2	0.3	0.2	19.5	0.1	0.2	0.1	39.2	0.2	0.1	0.2
SUBTOTAL	76.4	77.7	75.2	84.3	75.2	78	95.2	79	69	10.4	83.5	84.5	72.7	84	96.2	81.9	89.9	66.8

REST OF LC PHASES	23.6	22.3	24.8	15.7	24.8	22	4.8	21	31	89.6	16.5	15.5	27.3	16	3.8	18.1	10.1	33.2

Table S17. Contribution of each material (in %) to the total impacts of a 2 MW turbine in Ecoinvent.

	CC	EOF	FE	FET	FF	HOF	HT	HTn	IR	LO	ME	MET	OD	PMF	SO	TA	TET	WC
Steel	35.9	31.7	39.4	7.7	30.8	31.4	66.0	17.0	23.8	11.8	34.6	8.7	18.8	33.0	74.4	26.8	16.2	31.0
Copper	1.6	4.8	22.7	20.3	1.4	5.0	1.2	53.6	3.1	4.1	2.3	21.0	6.0	14.5	2.7	23.7	56.6	3.3
Chromium steel	5.6	4.5	4.1	1.1	4.6	4.6	12.3	3.1	6.8	3.0	2.5	1.3	4.4	9.3	3.8	5.2	12.7	3.5
Fibreglass	10.1	6.0	1.8	0.2	11.5	6.1	0.4	0.8	6.2	1.4	28.6	0.2	30.4	5.2	0.1	7.5	0.4	25.3
Concrete	8.5	7.9	2.4	0.4	4.9	8.1	0.4	2.0	2.6	3.9	1.7	0.5	3.5	3.9	0.6	4.9	2.5	2.3
Iron	2.9	2.7	2.5	0.4	2.7	2.7	10.9	1.2	2.1	0.8	1.3	0.5	1.5	2.6	7.0	2.1	1.2	1.4
SUBTOTAL	76.4	77.7	75.2	84.3	75.2	78	95.2	79	69	10.4	83.5	84.5	72.7	84	96.2	81.9	89.9	66.8
REST OF LC PHASES	23.6	22.3	24.8	15.7	24.8	22	4.8	21	31	89.6	16.5	15.5	27.3	16	3.8	18.1	10.1	33.2

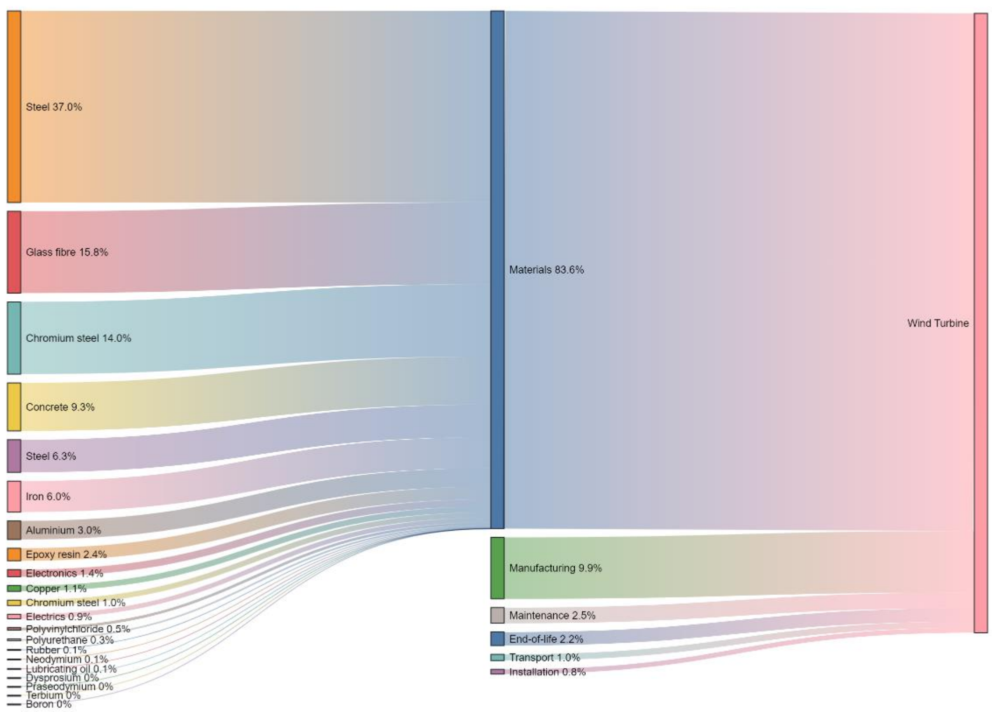

Figure S12. Contribution analysis of the Climate Change impact of a 2 MW turbine modelled with WindTrace.

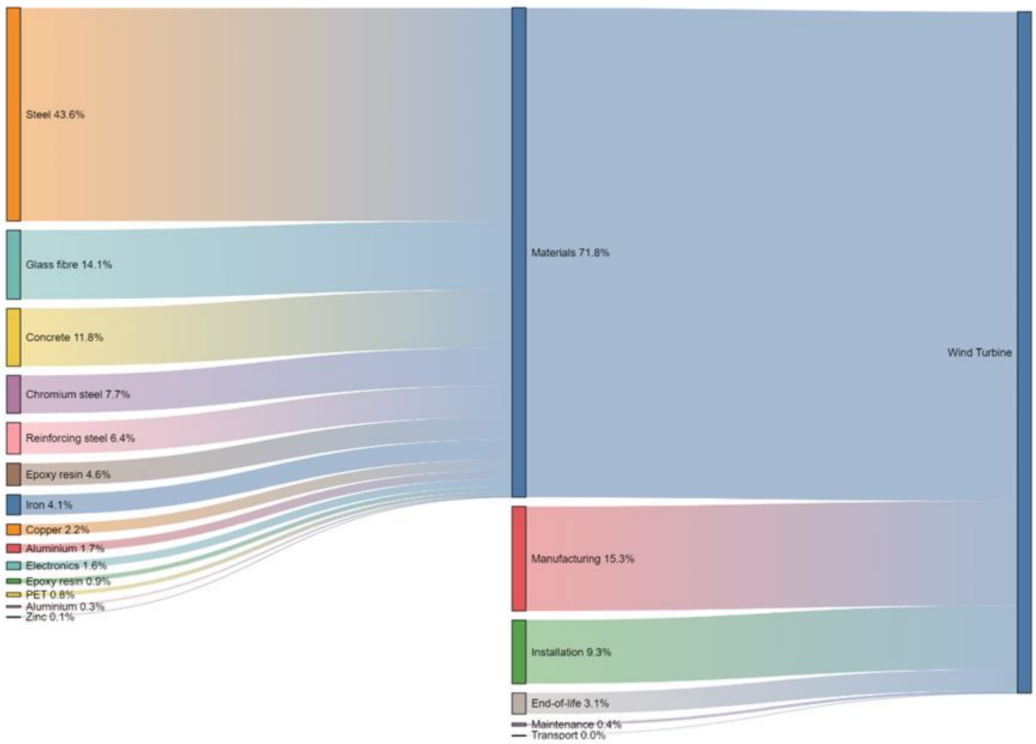

Figure S13. Contribution analysis of the Climate Change impact of an Ecoinvent 2 MW turbine.

4. Understanding the influence of sensitive parameters to the environmental impacts of wind turbines using WindTrace

4.1. Turbine parameters

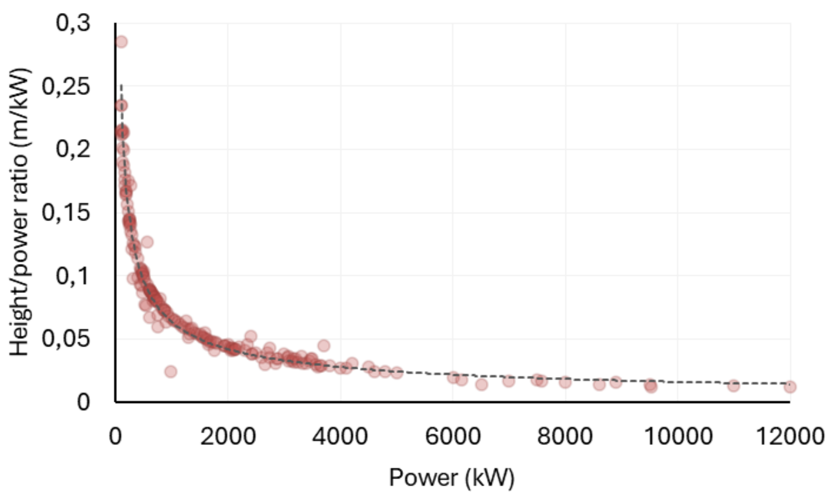

Figure S14. Hub height-to-power ratio of wind turbines in Europe in 2020.

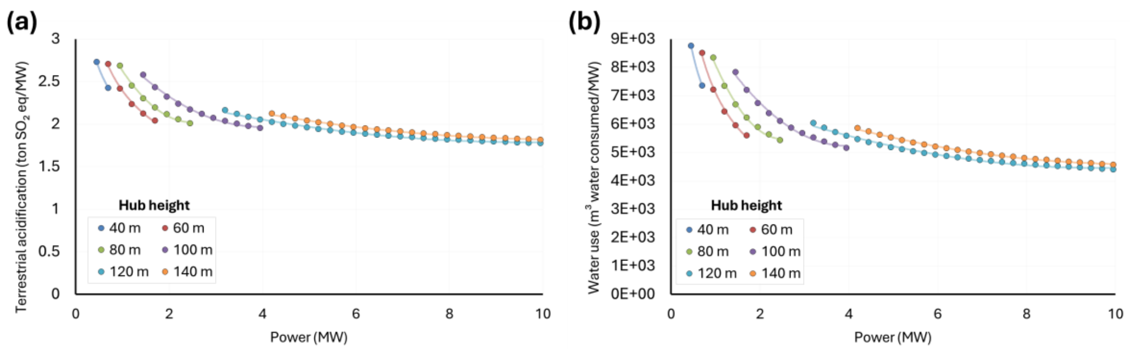

Figure S15. WindTrace results of (a) terrestrial acidification intensity (ton SO_2eq/MW) and (b) water use intensity (m^3 water consumed/MW) per turbine power for hub heights from 40 to 140 m.

- Generator type

The contribution of rare earth elements, particularly neodymium and praseodymium, to ionizing radiation impacts is markedly influenced by the selected life cycle impact assessment (LCIA) method. Under ReCiPe 2016, neodymium and praseodymium exhibit characterization factors for ionizing radiation that are approximately 150 and 236 times higher per kilogram, respectively, than that of steel. However, despite these high per-mass characterization factors, their absolute contribution to the ionizing radiation impact at the scale of a wind turbine remains limited due to the large disparity in mass between steel and rare earth elements.

For instance, in our 2 MW turbine case study (see Table S16), which uses a gearbox-based doubly-fed induction generator (DFIG), the total mass of steel is approximately 12,546 times greater than the combined mass of rare earths. Even when considering a drivetrain configuration with a direct-drive permanent magnet synchronous generator (PMSG), this ratio remains high, at approximately 836. Consequently, the impact of rare earths on the total ionizing radiation score is significantly diluted when considered at the full turbine level.

It is important to acknowledge that the choice of LCIA method substantially affects the magnitude of these impacts. For example, the Environmental Footprint (EF) v3.1 method assigns even higher characterization factors to rare earths, with neodymium exhibiting up to 797 times the ionizing radiation impact per kilogram compared to steel. This is primarily due to EF v3.1's higher characterization factor for Carbon-14 emissions to air, which are prominent in the life cycle inventories of neodymium and praseodymium. Specifically, EF v3.1 uses a Carbon-14 characterization factor that is approximately 8.7 times higher than that used in ReCiPe 2016, based on implementation details from Ecoinvent version 3.9.1.

Despite these differences, ReCiPe 2016 was selected as the LCIA method for this study to ensure consistency across all impact categories and to support comparative analysis. We recognize that this choice may result in a more conservative estimation of the ionizing radiation impacts associated with rare earths when compared to EF v3.1. This methodological sensitivity is noted here to contextualize the presented results and to provide transparency regarding the treatment of rare earth elements in the impact assessment.

4.2. Electricity parameters

- Lifetime

We took the 502 wind parks decommissioned in Europe until 2020 according to The Wind Power [42] and calculated their mean lifetime in months (Figure S16), which is of 18.9 years (226 months), with a standard deviation of 5.6 years (67.5 months).

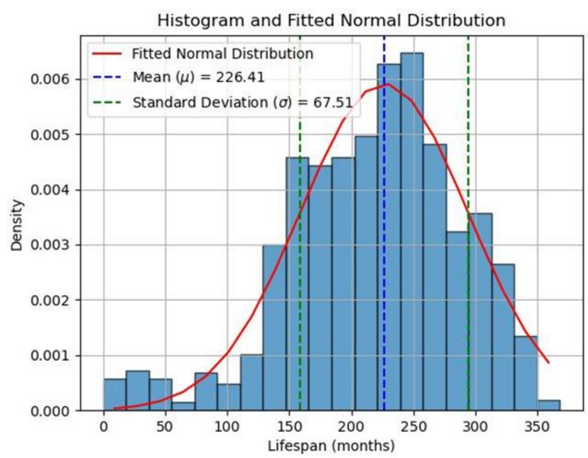

Figure S16. Lifetime histogram distribution of decommissioned wind parks in Europe until 2020.

- Capacity Factor

The parameters used in WindTrace to model the Reference Turbine, the 800 kW and the 4.5 MW turbines are listed in Table S18. Parameters employed in WindTrace to model the Reference Turbine, the 800 kW and the 4.5 MW turbines.Table S18. The capacity factors for the three specific turbines (Nordex-0.8MW, Vestas-2.0MW, and Enercon-4.5MW) was taken from renewables.ninja, in a location in Portugal where there is already a wind park (43.38948, 2.45054). Data displayed in Figure 7b in the main text fits to the equations listed in Table S19.

Table S18. Parameters employed in WindTrace to model the Reference Turbine, the 800 kW and the 4.5 MW turbines.

Turbine model	Parameter	Default value
Reference Turbine	Park power	2.0 MW
800 kW	Park power	0.8 MW
4.5 MW	Park power	4.5 MW
Common	Number of turbines	1
Common	Park location	DE (Germany)
Common	Park coordinates	53.4356, 11.2142 (Germany)
Common	Manufacturer	Vestas
Reference Turbine	Rotor diameter	90 m
800 kW	Rotor diameter	50 m
4.5 MW	Rotor diameter	113 m
Reference Turbine	Turbine power	2.0 MW
800 kW	Turbine power	0.8 MW
4.5 MW	Turbine power	4.5 MW
Reference Turbine	Hub height	97.14 m
800 kW	Hub height	50.6 m
4.5 MW	Hub height	120 m
Common	Commissioning year	2011
Common	Recycled steel share	Data from Eurofer (2012 – 2021)
Common	Electricity mix steel	Data from Ecoinvent considering country shares from Eurofer
Common	Generator type	Doubly fed induction generator with gearbox
Common	Lifetime	20 years
Common	Land use permanent intensity	3000 m^2/MW
Common	Land cover type	Pasture
Common	End-of-life scenario	Baseline

Table S19. Climate Change variation with capacity factor for 800 kW, 2 MW and 4.5 MW turbines modelled with WindTrace. The equations correspond to data displayed in Figure 7b in the main text.

Turbine model	Equation
800 kW	684.35/x
2 MW	418.73/x
4.5 MW	323.03/x

Table S20. Summary of climate change impacts per kWh, CF, rated power and operating years reported in theliterature, industry reports and databases. For those studies where the CF was not reported, we calculated it from the reported electricity production and lifetime, assuming no attrition rate, as follows: $\frac{\text{Anual electricity production (MWh)} \times 365 \text{ days} \times 24 \text{ hours}}{\text{Rated capacity (MW)}}$.

Authors	Operating years	Rated capacity per turbine (kW)	CF (%)	Climate change (g CO_{2eq}/kWh)
Vestas [21]	20	6200	39.7	6.2
Vestas [20]	20	6000	41.9	5.6
Ecoinvent [43]	20	4500	18.3	33.8
	20	2000	18.3	20.0
	20	800	18.3	19.1
Vestas [19]	20	4200	39.9	7.3

Vestas [17]	20	4200	43.0	5.6
Vestas [18]	20	4200	47.3	4.4
Vestas [16]	20	3450	43.8	7.6
Vestas [15]	20	3450	47.5	6.4
Vestas [14]	20	3450	53.6	5.1
Vestas [11]	20	3300	37.2	8.2
Vestas [10]	20	3300	42.4	6.4
Lundie et al. [44]	-	3250	35.8	18.3
	-	2250	34.0	14.1
	-	2250	48.7	11.7
	-	2250	46.2	18.0
Bonou et al. [45]	20	3200	51.4	5.0
	20	2300	55.4	6.0
Demir and Taşkin [46]	20	3020	15.1	22.3
	20	2050	22.1	16.2
Schreiber et al. [47]	20	3000	30.4	7.3
	20	3000	30.4	12.4
Gomaa et al. [48]	20	3000	25.7	9.1
Vestas [49]	20	3000	29.3	7.0
Vestas [6]	20	2600	38.4	7.9
Zhuo et al. [50]	20	2500	30.0	10.4
	20	2500	30.0	8.5
Ozsahin et al. [51]	25	2500	39.3	5.2
Chipindula et al. [52]	20	2300	35.0	5.6
	20	2000	35.0	6.9
	20	1000	35.0	7.1
Rossi et al. [53]	30	2000	26.7	29.8
	30	2000	26.7	22.0
Alsaleh and Sattler [54]	20	2000	16.8	52.7
	25	2000	16.8	42.2
	30	2000	16.8	35.3
Wang et al. [55]	20	2000	32.2	22.8
Ji and Chen [56]	21	2000	25.8	5.7
Vestas [5]	20	2000	50.2	6.7
Vestas [57]	20	2000	43.2	7.2
Verma et al. [58]	20	1650	24.0	11.3
Vélez-Henao and Vivanco [59]	20	1650	42.0	12.9
Al-Behadili and El-Osta [60]	20	1650	42.4	10.4
Liu et al. [61]	20	1500	32.8	6.6
Teffera et al. [62]	20	1500	17.0	36.4
	20	1500	32.0	28.6

	20	1500	24.0	36.0
Oebels and Pacca [63]	20	1500	34.3	7.1
Gao et al. [64]	20	1500	31.8	5.2
Ozoemena et al. [65]	25	1500	21.0	16.6
	25	1500	22.0	10.3
Kumar et al. [66]	25	1500	31.1	18.7
Xu et al. [67]	20	750-1500	30.0	8.6
Ardente et al. [68]	20	660	19.0	14.8
Oğuz and Şentürk [69]	20	600	38.1	10.6
Kabir et al. [70]	25	100	24.0	17.8
	25	20	22.0	25.1
	25	5	23.0	42.7

5. References

[1] Vestas. Life Cycle Assessment of Electricity Production from a V90-2.0MW Wind Plant. 2011.

[2] Vestas. Life Cycle Assessment of Electricity Production from an onshore V100-2.0MW Wind Plant. 2015.

[3] Vestas. Life Cycle Assessment of Electricity Production from an onshore V110-2.0MW Wind Plant. 2015.

[4] Vestas. Life Cycle Assessment of Electricity Production from an onshore V116-2.0MW Wind Plant. 2018.

[5] Vestas. Life Cycle Assessment of Electricity Production from an onshore V120-2.0 MW Wind Plant. 2018.

[6] Vestas. Life Cycle Assessment of Electricity Production from an onshore V100-2.6MW Wind Plant. 2013.

[7] Vestas. Life Cycle Assessment of Electricity Production from an onshore V90-3.0 MW Wind Plant. 2012.

[8] Vestas. Life Cycle Assessment of Electricity Production from an onshore V105-3.3 MW Wind Plant. 2014.

[9] Vestas. Life Cycle Assessment of Electricity Production from an onshore V112-3.3 MW Wind Plant. 2018.

[10] Vestas. Life Cycle Assessment of Electricity Production from an onshore V117-3.3 MW Wind Plant. 2014.

[11] Vestas. Life Cycle Assessment of Electricity Production from an onshore V126-3.3 MW Wind Plant. 2014.

[12] Vestas. Life Cycle Assessment of Electricity Production from an onshore V105-3.45 MW Wind Plant. 2017.

[13] Vestas. Life Cycle Assessment of Electricity Production from an onshore V112-3.45 MW Wind Plant. 2017.

[14] Vestas. Life Cycle Assessment of Electricity Production from an onshore V117-3.45 MW Wind Plant. 2017.

[15] Vestas. Life Cycle Assessment of Electricity Production from an onshore V126-3.45 MW Wind Plant. 2017.

[16] Vestas. Life Cycle Assessment of Electricity Production from an onshore V136-3.45 MW Wind Plant. 2017.
[17] Vestas. Life Cycle Assessment of electricity production from an onshore V117-4.2MW Wind Plant. 2019.
[18] Vestas. Life Cycle Assessment of Electricity Production from an onshore V136-4.2 MW Wind Plant. 2022.
[19] Vestas. Life Cycle Assessment of Electricity Production from an onshore V150-4.2 MW Wind Plant. 2022.
[20] Vestas. Life Cycle Assessment of Electricity Production from an onshore V150-6.0 MW Wind Plant. 2023.
[21] Vestas. Life Cycle Assessment of Electricity Production from an onshore V162-6.2 MW Wind Plant. 2023.
[22] Psomopoulos CS, Kalkanis K, Kaminaris S, Ioannidis GC, Pachos P. A review of the potential for the recovery of wind turbine blade waste materials. Recycling 2019;4. https://doi.org/10.3390/recycling4010007.
[23] Carrara S, Alves Dias P, Plazzotta B, Pavel C. Raw materials demand for wind and solar PV technologies in the transition towards a decarbonised energy system, EUR 30095 EN. Luxembourg: Publications Office of the European Union; 2020. https://doi.org/10.2760/160859.
[24] Mutel C. Brightway: An open source framework for Life Cycle Assessment. J Open Source Softw 2017;2:236. https://doi.org/10.21105/JOSS.00236.
[25] LM Wind Power. Blade Material Passport LM 37.3 P2. 2022.
[26] Vestas. Material Passport Wind Turbine Blade V47. 2022.
[27] Huijbregts MAJ, Steinmann ZJN, Elshout PMF, Stam G, Verones F, Vieira M, et al. ReCiPe2016: a harmonised life cycle impact assessment method at midpoint and endpoint level. International Journal of Life Cycle Assessment 2017;22:138–47. https://doi.org/10.1007/s11367-016-1246-y.
[28] Eurofer. European Steel in Figures 2022. 2022.
[29] Denholm P, Hand M, Jackson M, Ong S. Land-use requirements of modern wind power plants in the United States. vol. Technical. National Renewable Energy Laboratory; 2009.
[30] Siemens Gamesa. Electricity from a European onshore wind farm using SG 6.2-170 / SG 6.6-170 wind turbines. 2022.
[31] Malachy Walsh and Partners. Environmental Impact Assessment Report. Drumnahough Wind Farm. Chapter 3: Civil Engineering. 2020.
[32] Bang J-I, Ma C, Tarantino E, Vela A, Yamane D, Suh S, et al. Life Cycle Assessment of Greenhouse Gas Emissions for Floating Offshore Wind Energy in California Committee in charge. 2019.
[33] Li C, Mogollón JM, Tukker A, Dong J, von Terzi D, Zhang C, et al. Future material requirements for global sustainable offshore wind energy development. Renewable and Sustainable Energy Reviews 2022;164. https://doi.org/10.1016/j.rser.2022.112603.
[34] Jensen JP. Evaluating the environmental impacts of recycling wind turbines. Wind Energy 2019;22:316–26. https://doi.org/10.1002/we.2287.
[35] Diez-Cañamero B, Mendoza JMF. Circular economy performance and carbon footprint of wind turbine blade waste management alternatives. Waste Management 2023;164:94–105. https://doi.org/10.1016/j.wasman.2023.03.041.

[36] Tam VWY, Soomro M, Evangelista ACJ. A review of recycled aggregate in concrete applications (2000–2017). Constr Build Mater 2018;172:272–92. https://doi.org/10.1016/j.conbuildmat.2018.03.240.
[37] Nexans. Nexans. 19/33kV Three Core 3C 120mm2 19/33kV PVC Black n.d. https://www.nexans.com.au/en/products/Medium-Voltage/MV-XLPE-Three-Core/19-33kV-Th25769.html (accessed September 16, 2024).
[38] ABB. Cuaderno de aplicaciones técnicas nº 12. Plantas eólicas. 2012.
[39] McKenna R, Pfenninger S, Heinrichs H, Schmidt J, Staffell I, Bauer C, et al. High-resolution large-scale onshore wind energy assessments: A review of potential definitions, methodologies and future research needs. Renew Energy 2022;182:659–84. https://doi.org/10.1016/j.renene.2021.10.027.
[40] ABB Transformers AB. Environmental Product Declaration Power transformer TrafoStar 500 MVA. 2000.
[41] Sacchi R, Besseau R, Pérez-López P, Blanc I. Exploring technologically, temporally and geographically-sensitive life cycle inventories for wind turbines: A parameterized model for Denmark. Renew Energy 2019;132:1238–50. https://doi.org/10.1016/j.renene.2018.09.020.
[42] Pierrot M. World wind farms database 2021.
[43] Wernet G, Bauer C, Steubing B, Reinhard J, Moreno-Ruiz E, Weidema B. The ecoinvent database version 3 (part I): Overview and methodology. International Journal of Life Cycle Assessment 2016;21:1218–30. https://doi.org/10.1007/s11367-016-1087-8.
[44] Lundie S, Wiedmann T, Welzel M, Busch T. Global supply chains hotspots of a wind energy company. J Clean Prod 2019;210:1042–50. https://doi.org/10.1016/j.jclepro.2018.10.216.
[45] Bonou A, Laurent A, Olsen SI. Life cycle assessment of onshore and offshore wind energy-from theory to application. Appl Energy 2016;180:327–37. https://doi.org/10.1016/j.apenergy.2016.07.058.
[46] Demir N, Taşkin A. Life cycle assessment of wind turbines in Pınarbaşı-Kayseri. J Clean Prod 2013;54:253–63. https://doi.org/10.1016/j.jclepro.2013.04.016.
[47] Schreiber A, Marx J, Zapp P. Comparative life cycle assessment of electricity generation by different wind turbine types. J Clean Prod 2019;233:561–72. https://doi.org/10.1016/j.jclepro.2019.06.058.
[48] Gomaa MR, Rezk H, Mustafa RJ, Al-Dhaifallah M. Evaluating the environmental impacts and energy performance of a wind farm system utilizing the life-cycle assessment method: A practical case study. Energies (Basel) 2019;12. https://doi.org/10.3390/en12173263.
[49] Vestas. Life Cycle Assessment of Electricity Production from an onshore V112-3.0 MW Wind Plant. 2011.
[50] Zhuo ZY, Chen MJ, Li XY. A comparative analysis of carbon reduction potential for directly driven permanent magnet and doubly fed asynchronous wind turbines. Energy Sci Eng 2023;11:978–88. https://doi.org/10.1002/ese3.1425.
[51] Ozsahin B, Elginoz N, Germirli Babuna F. Life cycle assessment of a wind farm in Turkey. Environmental Science and Pollution Research 2022;29:71000–13. https://doi.org/10.1007/s11356-022-20783-0.

[52] Chipindula J, Botlaguduru VSV, Du H, Kommalapati RR, Huque Z. Life cycle environmental impact of onshore and offshore wind farms in Texas. Sustainability (Switzerland) 2018;10. https://doi.org/10.3390/su10062022.
[53] Rossi F, Zuffi C, Parisi ML, Fiaschi D, Manfrida G. Comparative scenario-based LCA of renewable energy technologies focused on the end-of-life evaluation. J Clean Prod 2023;405. https://doi.org/10.1016/j.jclepro.2023.136931.
[54] Alsaleh A, Sattler M. Comprehensive life cycle assessment of large wind turbines in the US. Clean Technol Environ Policy 2019;21:887–903. https://doi.org/10.1007/s10098-019-01678-0.
[55] Wang S, Wang S, Liu J. Life-cycle green-house gas emissions of onshore and offshore wind turbines. J Clean Prod 2019;210:804–10. https://doi.org/10.1016/j.jclepro.2018.11.031.
[56] Ji S, Chen B. Carbon footprint accounting of a typical wind farm in China. Appl Energy 2016;180:416–23. https://doi.org/10.1016/j.apenergy.2016.07.114.
[57] Vestas. Life Cycle Assessment of Electricity Production from an onshore V110-2.0 MW Wind Plant. 2015.
[58] Verma S, Paul AR, Haque N. Selected Environmental Impact Indicators Assessment of Wind Energy in India Using a Life Cycle Assessment. Energies (Basel) 2022;15. https://doi.org/10.3390/en15113944.
[59] Vélez-Henao JA, Vivanco DF. Hybrid life cycle assessment of an onshore wind farm including direct and indirect services: A case study in Guajira, Colombia. J Environ Manage 2021;284. https://doi.org/10.1016/j.jenvman.2021.112058.
[60] Al-Behadili SH, El-Osta WB. Life Cycle Assessment of Dernah (Libya) wind farm. Renew Energy 2015;83:1227–33. https://doi.org/10.1016/j.renene.2015.05.041.
[61] Liu P, Liu L, Xu X, Zhao Y, Niu J, Zhang Q. Carbon footprint and carbon emission intensity of grassland wind farms in Inner Mongolia. J Clean Prod 2021;313. https://doi.org/10.1016/j.jclepro.2021.127878.
[62] Teffera B, Assefa B, Björklund A, Assefa G. Life cycle assessment of wind farms in Ethiopia. International Journal of Life Cycle Assessment 2021;26:76–96. https://doi.org/10.1007/s11367-020-01834-5.
[63] Oebels KB, Pacca S. Life cycle assessment of an onshore wind farm located at the northeastern coast of Brazil. Renew Energy 2013;53:60–70. https://doi.org/10.1016/j.renene.2012.10.026.
[64] Gao, C. kang, Na, H. ming, Song, K. hui, Dyer, N., Tian, F., Xu, Q. jiang, & Xing, Y. hong. (2019). Environmental impact analysis of power generation from biomass and wind farms in different locations. Renewable and Sustainable Energy Reviews, 102, 307–317. https://doi.org/10.1016/j.rser.2018.12.018.
[65] Ozoemena M, Cheung WM, Hasan R. Comparative LCA of technology improvement opportunities for a 1.5-MW wind turbine in the context of an onshore wind farm. Clean Technol Environ Policy 2018;20:173–90. https://doi.org/10.1007/s10098-017-1466-2.
[66] Kumar I, Tyner WE, Sinha KC. Input-output life cycle environmental assessment of greenhouse gas emissions from utility scale wind energy in the United States. Energy Policy 2016;89:294–301. https://doi.org/10.1016/j.enpol.2015.12.004.
[67] Xu L, Pang M, Zhang L, Poganietz WR, Marathe SD. Life cycle assessment of onshore wind power systems in China. Resour Conserv Recycl 2018;132:361–8. https://doi.org/10.1016/j.resconrec.2017.06.014.

[68] Ardente F, Beccali M, Cellura M, Lo Brano V. Energy performances and life cycle assessment of an Italian wind farm. Renewable and Sustainable Energy Reviews 2008;12:200–17. https://doi.org/10.1016/j.rser.2006.05.013.
[69] Oğuz E, Şentürk AE. Selection of the most sustainable renewable energy system for Bozcaada Island: Wind vs. Photovoltaic. Sustainability (Switzerland) 2019;11. https://doi.org/10.3390/su11154098.
[70] Kabir MR, Rooke B, Dassanayake GDM, Fleck BA. Comparative life cycle energy, emission, and economic analysis of 100 kW nameplate wind power generation. Renew Energy 2012;37:133–41. https://doi.org/10.1016/j.renene.2011.06.003.
[71] Razali, N. M., & Wah, Y. B. (2011). Power comparisons of Shapiro-Wilk, Kolmogorov-Smirnov, Lilliefors and Anderson-Darling tests. Journal of Statistical Modeling and Analytics, 2(1), 21–33.
[72] Wilcox, R. R. (2010). Fundamentals of Modern Statistical Methods: Substantially Improving Power and Accuracy. Springer. https://doi.org/10.1007/978-1-4419-5525-8.